

6. Black Holes

Black holes are among the most enigmatic objects in the universe. They are described by deceptively simple solutions to the Einstein equations, yet hold a host of insights and surprises, from the meaning of causal structure, to connections to thermodynamics and, ultimately, quantum gravity. The purpose of this section is to begin to uncover some of the mysteries of these wonderful objects.

6.1 The Schwarzschild Solution

We have already met the simplest black hole solution back in Section 1.3: this is the Schwarzschild solution, with metric

$$ds^2 = - \left(1 - \frac{2GM}{r}\right) dt^2 + \left(1 - \frac{2GM}{r}\right)^{-1} dr^2 + r^2(d\theta^2 + \sin^2 \theta d\phi^2) \quad (6.1)$$

It is not hard to show that this solves the vacuum Einstein equations $R_{\mu\nu} = 0$. Indeed, the calculations can be found in Section 4.2 where we first met de Sitter space. The Schwarzschild solution is a special case of the more general metric (4.9) with $f(r)^2 = 1 - 2GM/r$ and it's simple to check that this obeys the Einstein equation which, as we've seen, reduces to the simple differential equations (4.10) and (4.11).

M is for Mass

The Schwarzschild solution depends on a single parameter, M , which should be thought of as the mass of the black hole. This interpretation already follows from the relation to Newtonian gravity that we first discussed way back in Section 1.2 where we anticipated that the g_{00} component of the metric should be (1.26)

$$g_{00} = -(1 + 2\Phi)$$

with Φ the Newtonian potential. We made this intuition more precise in Section 5.1.2 where we discussed the Newtonian limit. For the Schwarzschild metric, we clearly have

$$\Phi = -\frac{GM}{r}$$

which is indeed the Newtonian potential for a point mass M at the origin.

The black hole also provides an opportunity to roadtest the technology of Komar integrals developed in Section 4.3.3. The Schwarzschild spacetime admits a timelike Killing vector $K = \partial_t$. The dual one-form is then

$$K = g_{00}dt = - \left(1 - \frac{2GM}{r}\right) dt$$

Following the steps described in Section 4.3.3, we can then construct the 2-form

$$F = dK = -\frac{2GM}{r^2} dr \wedge dt$$

which takes a form similar to that of an electric field, with the characteristic $1/r^2$ fall-off. The Komar integral instructs us to compute the mass by integrating

$$M_{\text{Komar}} = -\frac{1}{8\pi G} \int_{\mathbf{S}^2} \star F$$

where \mathbf{S}^2 is any sphere with radius larger than the horizon $r = 2GM$. It doesn't matter which radius we choose; they all give the same answer, just like all Gaussian surfaces outside a charge distribution give the same answer in electromagnetism. Since the area of a sphere at radius r is $4\pi r^2$, the integral gives

$$M_{\text{Komar}} = M$$

for the Schwarzschild black hole.

There's something a little strange about the Komar mass integral. As we saw in Section 4.3.3, the 2-form $F = dK$ obeys something very similar to the Maxwell equations, $d\star F = 0$. But these are the vacuum Maxwell equations in the absence of any current, so we would expect any "electric charge" to vanish. Yet this "electric charge" is precisely the mass M_{Komar} which, as we have seen, is distinctly not zero. What's happening is that, for the black hole, the mass is all localised at the origin $r = 0$, where the field strength F diverges.

We might expect that the Schwarzschild solution only describes something physically sensible when $M \geq 0$. (The $M = 0$ Schwarzschild solution is simply Minkowski space-time.) However, the metric (6.1) is a solution of the Einstein equations for all values of M . As we proceed, we'll see that the $M < 0$ solution does indeed have some rather screwy features that make it unphysical.

6.1.1 Birkhoff's Theorem

The Schwarzschild solution (6.1) is, it turns out, the unique spherically symmetric, asymptotically flat solution to the vacuum Einstein equations. This is known as the *Birkhoff theorem*. In particular, this means that the Schwarzschild solution does not just describe a black hole, but it describes the spacetime outside any non-rotating, spherically symmetric object, like a star.

Here we provide a sketch of the proof. The first half of the proof involves setting up a useful set of coordinates. First, we make use of the statement that the metric is spherically symmetric, which means that it has an $SO(3)$ isometry. One of the more fiddly parts of the proof is to show that any metric with such an isometry can be written in coordinates that make this isometry manifest,

$$ds^2 = g_{\tau\tau}(\tau, \rho)d\tau^2 + 2g_{\tau\rho}(\tau, \rho)d\tau d\rho + g_{\rho\rho}(\tau, \rho) d\rho^2 + r^2(\tau, \rho) d\Omega_2^2$$

Here τ and ρ are some coordinates and $d\Omega_2^2$ is the familiar metric on \mathbf{S}^2

$$d\Omega_2^2 = d\theta^2 + \sin^2 \theta d\phi^2$$

The $SO(3)$ isometry then acts on this \mathbf{S}^2 in the usual way, leaving τ and ρ untouched. This is said to be a *foliation* of the space by the spheres \mathbf{S}^2 .

The size of the sphere is determined by the function $r(\tau, \rho)$ in the above metric. The next step in the proof is to change coordinates so that we work with τ and r , rather than τ and ρ . We're then left with the metric

$$ds^2 = g_{\tau\tau}(\tau, r)d\tau^2 + 2g_{\tau r}(\tau, r)d\tau dr + g_{rr}(\tau, r) dr^2 + r^2 d\Omega_2^2$$

In fact there's a subtlety in the argument above: for some functions $r(\tau, \rho)$, it's not possible to exchange ρ for r . Examples of such functions include $r = \text{constant}$ and $r = \tau$. We can rule out such counter-examples by insisting that asymptotically the spacetime looks like Minkowski space.

Our next step is to introduce a new coordinate that gets rid of the cross-term $g_{\tau r}$. To this end, consider the a coordinate $\tilde{t}(\tau, r)$. Then

$$d\tilde{t}^2 = \left(\frac{\partial\tilde{t}}{\partial\tau}\right)^2 d\tau^2 + 2\frac{\partial\tilde{t}}{\partial\tau}\frac{\partial\tilde{t}}{\partial r}d\tau dr + \left(\frac{\partial\tilde{t}}{\partial r}\right)^2 dr^2$$

We can always pick a choice of $\tilde{t}(\tau, r)$ so that the cross-term $g_{\tau r}$ vanishes in the new coordinates. We're then left with the simpler looking metric,

$$ds^2 = -f(\tilde{t}, r) d\tilde{t}^2 + g(\tilde{t}, r) dr^2 + r^2 d\Omega_2^2$$

Where we've now included the expected minus sign in the temporal part of the metric, reflecting our chosen signature. This is as far as we can go making useful coordinate choices. To proceed, we need to use the Einstein equations. As always, this involves sitting down and doing a fiddly calculation. Here we present only the (somewhat surprising) conclusion: the vacuum Einstein equations require that

$$f(r, \tilde{t}) = f(r)h(\tilde{t}) \quad \text{and} \quad g(r, \tilde{t}) = g(r)$$

In other words, the metric takes the form

$$ds^2 = -f(r)h(\tilde{t})d\tilde{t}^2 + g(r)dr^2 + r^2 d\Omega_2^2$$

But we can always absorb that $h(\tilde{t})$ factor by redefining the time coordinate, so that $h(\tilde{t})d\tilde{t}^2 = dt^2$. Finally, we're left with the a metric of the form

$$ds^2 = -f(r)dt^2 + g(r)dr^2 + r^2 d\Omega_2^2 \tag{6.2}$$

This is important. We assumed that the metric was spherically symmetric, but made no such assumption about the lack of time dependence. Yet the Einstein equations have forced this upon us, and the final metric (6.2) has two sets of Killing vectors. The first arises from the $SO(3)$ isometry that we originally assumed, but the second is the timelike Killing vector $K = \partial_t$ that has emerged from the calculation.

At this point we need to finish solving the Einstein equations. It turns out that they require $f(r) = g(r)^{-1}$, so the metric (6.2) reduces to the simple ansatz (4.9) that we considered previously. The Schwarzschild solution (6.1) is the most general solution to the Einstein equations with vanishing cosmological constant.

The fact that we assumed only spherical symmetry, and not time independence, means that the Schwarzschild solution not only describes the spacetime outside a time-independent star, but also outside a collapsing star, providing that the collapse is spherically symmetric.

A Closer Look at Time Independence

There are actually two, different meanings to “time independence” in general relativity.

A spacetime is said to be *stationary* if it admits an everywhere timelike Killing vector field K . In asymptotically flat spacetimes, we usually normalise this so that $K^2 \rightarrow -1$ asymptotically.

A spacetime is said to be *static* if it is stationary and, in addition, is invariant under $t \rightarrow -t$, where t is a coordinate along the integral curves of K . In particular, this rules out $dt dX$ cross-terms in the metric, with X some other coordinate.

Birkhoff’s theorem tells us that spherical symmetry implies that the spacetime is necessarily static. In Section 6.3, we’ll come across spacetimes that are stationary but not static.

6.1.2 A First Look at the Horizon

There are two values of r where the Schwarzschild metric goes bad: $r = 0$ and $r = 2GM$. At each of these values, one of the components of the metric diverges but, as we will see, the interpretation of this divergence is rather different in the two cases. We will learn that the divergence at the point $r = 0$ is because the spacetime is sick: this point is called the *singularity*. The theory of general relativity breaks down as we get close to the singularity and to make sense of what's happening there we need to turn to a quantum theory of spacetime.

In contrast, nothing so dramatic happens at the surface $r = 2GM$ and the divergence in the metric is merely because we've made a poor choice of coordinates: this surface is referred to as the *event horizon*, usually called simply the *horizon*. Many of the surprising properties of black holes lie in interpreting the event horizon.

There is a simple diagnostic to determine whether a divergence in the metric is due to a true singularity of the spacetime, or to a poor choice of coordinates. We build a scalar quantity that does not depend on the choice of coordinates. If this too diverges then it's telling us that the spacetime itself is indeed sick at that point. If it does not diverge, we can't necessarily conclude that the spacetime isn't sick because there may be some other scalar quantity that signifies there is a problem. Nonetheless, we might start to wonder if perhaps nothing very bad happens.

The simplest scalar is, of course, the Ricci scalar. But this is necessarily $R = 0$ for any vacuum solution to the Einstein equation so it is not helpful in detecting the nature of singularities. The same is true for $R_{\mu\nu}R^{\mu\nu}$. For this reason, the simplest curvature diagnostic is the *Kretschmann scalar*, $R^{\mu\nu\rho\sigma}R_{\mu\nu\rho\sigma}$. For the Schwarzschild solution it is given by

$$R^{\mu\nu\rho\sigma}R_{\mu\nu\rho\sigma} = \frac{48G^2M^2}{r^6} \quad (6.3)$$

We see that the Kretschmann scalar exhibits no pathology at the surface $r = 2GM$, where $R^{\mu\nu\rho\sigma}R_{\mu\nu\rho\sigma} \sim 1/(GM)^4$. This suggests that perhaps this divergence in the metric isn't as worrisome as it may have first appeared. Note, moreover, that, perhaps counter-intuitively, heavier black holes have smaller curvature at the horizon. We see that this arises because such black holes are bigger and the $1/r^6$ factor beats the M^2 factor.

In contrast, the curvature indeed diverges at the origin $r = 0$, telling us that the spacetime is problematic at this point. Of course, given that we have still to understand

the horizon at $r = 2GM$, it's not entirely clear that we can trust the Schwarzschild metric for values $r < 2GM$. As we will proceed, we will see that the singularity at $r = 0$ is a genuine feature of the (classical) black hole.

The Near Horizon Limit: Rindler Space

To understand what's happening near the horizon $r = 2GM$, we can zoom in and look at the metric in the vicinity of the horizon. To do this, we write

$$r = 2GM + \eta$$

where we take $\eta \ll 2GM$. We further take $\eta > 0$ which means that we're looking at the region of spacetime just outside the horizon. We then approximate the components of the metric as

$$1 - \frac{2GM}{r} \approx \frac{\eta}{2GM} \quad \text{and} \quad r^2 = (2GM + \eta)^2 \approx (2GM)^2$$

To this order, the Schwarzschild metric becomes

$$ds^2 = -\frac{\eta}{2GM} dt^2 + \frac{2GM}{\eta} d\eta^2 + (2GM)^2 d\Omega_2^2$$

The first thing that we see is that the metric has decomposed into a direct product of an \mathbf{S}^2 of radius $2GM$, and a $d = 1 + 1$ dimensional Lorentzian geometry. We'll focus on this 2d Lorentzian geometry. We make the change of variables

$$\rho^2 = 8GM\eta$$

after which the 2d metric becomes

$$ds^2 = -\left(\frac{\rho}{4GM}\right)^2 dt^2 + d\rho^2$$

This rather simple metric is known as *Rindler space*. It is, in fact, just Minkowski space in disguise. The disguise is the transformation

$$T = \rho \sinh\left(\frac{t}{4GM}\right) \quad \text{and} \quad X = \rho \cosh\left(\frac{t}{4GM}\right) \quad (6.4)$$

after which the metric becomes

$$ds^2 = -dT^2 + dX^2 \quad (6.5)$$

We've met something very similar to the coordinates (6.4) previously: they are the coordinates experienced by an observer undergoing constant acceleration $a = 1/4GM$, where t is the proper time of this observer. (We saw such coordinates earlier in (1.25) which differ only by a constant offset to the spatial variable ρ .) This makes sense: an observer who sits at a constant ρ value, corresponding to a constant r value, must accelerate in order to avoid falling into the black hole.

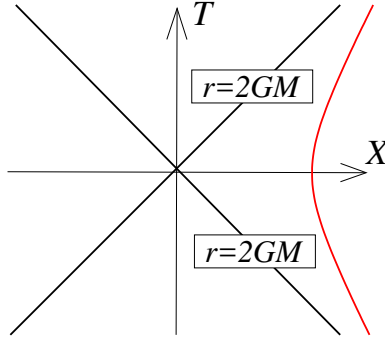


Figure 43: The near horizon limit of a black hole is Rindler spacetime, with the null lines $X = \pm T$ corresponding to the horizon at $r = 2GM$. Also shown in red is a line of constant $r > 2GM$ outside the black hole.

We can now start to map out what part of Minkowski space (6.5) corresponds to the outside of the black hole horizon. This is $\rho > 0$ and $t \in (-\infty, +\infty)$. From the change of variables (6.4), we see that this corresponds to the region $X > |T|$.

We can also see what becomes of the horizon itself. This sits at $r = 2GM$, or $\rho = 0$. For any finite t , the horizon $\rho = 0$ gets mapped to the origin of Minkowski space, $X = T = 0$. However, the time coordinate is degenerate at the horizon since $g_{00} = 0$. If we scale $t \rightarrow \infty$, and $\rho \rightarrow 0$ keeping the combination $\rho e^{\pm t/4GM}$ fixed, then we see that the horizon actually corresponds to the lines:

$$r = 2GM \quad \Rightarrow \quad X = \pm T$$

This is our first lesson. The event horizon of a black hole is not a timelike surface, like the surface of a star. Instead it is a null surface. This is depicted in Figure 43.

Although our starting point was restricted to coordinates X and T given by (6.4), once we get to the Minkowski space metric (6.5) there's no reason to retain this restriction. Indeed, clearly the metric makes perfect sense if we extend the range of the coordinates to $X, T \in \mathbf{R}$. Moreover, this metric makes it clear that nothing fishy is happening at the horizon $X = \pm|T|$. We see that if we zoom in on the horizon, then it's no different from any other part of spacetime. Nonetheless, as we go on we will learn that the horizon does have some rather special properties, but you only get to see them if you look at things from a more global perspective.

6.1.3 Eddington-Finkelstein Coordinates

Above we saw that, in the near-horizon limit, a clever change of variables allows us

to remove the coordinate singularity at the horizon and extend the spacetime beyond. Our goal in this section is to play the same game, but now for the full black hole metric.

Before we proceed, it's worth commenting on the logic here. When we first met differential geometry in Section 2, we made a big deal of the fact that a single set of coordinates need not cover the entire manifold. Instead, one typically needs different coordinates in different patches, together with transition functions that relate the coordinates where the patches overlap. The situation with the black hole is similar, but not quite the same. It's true that the coordinates of the Schwarzschild metric (6.1) do not cover the entire spacetime: they break down at $r = 2GM$ and it's not clear that we should trust the metric for $r < 2GM$. But rather than finding a new set of coordinates in the region beyond the horizon, and trying to patch this together with our old coordinates, we're instead going to find a new set of coordinates that works everywhere.

Our first step is to introduce a new radial coordinate, r_* , defined by

$$dr_*^2 = \left(1 - \frac{2GM}{r}\right)^{-2} dr^2 \quad (6.6)$$

The solution to this differential equation is straightforward to find: it is

$$r_* = r + 2GM \log\left(\frac{r - 2GM}{2GM}\right) \quad (6.7)$$

We see that the region outside the horizon $2GM < r < \infty$ maps to $-\infty < r_* < +\infty$ in the new coordinate. As we approach the horizon, the change in r is increasingly slow as we vary r_* (since $dr/dr_* \rightarrow 0$ as $r \rightarrow 2GM$.) For this reason it is called the *tortoise* coordinate. (It is also sometimes called the Regge-Wheeler radial coordinate.)

The tortoise coordinate is well adapted to describe the path of light rays travelling in the radial direction. Such light rays follow curves satisfying

$$ds^2 = 0 \quad \Rightarrow \quad \frac{dr}{dt} = \pm \left(1 - \frac{2GM}{r}\right) \quad \Rightarrow \quad \frac{dr_*}{dt} = \pm 1$$

We see that null, radial geodesics are given by

$$t \pm r_* = \text{constant}$$

where the plus sign corresponds to ingoing geodesics (as t increases, r_* must decrease) and the negative sign to outgoing geodesics.

Next, we introduce a pair of null coordinates

$$v = t + r_\star \quad \text{and} \quad u = t - r_\star$$

In what follows we will consider the Schwarzschild metric written first in coordinates (v, r) , then in coordinates (u, r) and finally, in Section 6.1.4, in coordinates (u, v) .

Ingoing Eddington-Finkelstein Coordinates

As a first attempt to extend the Schwarzschild solution beyond the horizon, we replace t with $t = v - r_\star(r)$. We have

$$dt = dv - dr_\star = dv - \left(1 - \frac{2GM}{r}\right)^{-1} dr$$

Making this substitution in the Schwarzschild metric (6.1), we find the new metric

$$ds^2 = - \left(1 - \frac{2GM}{r}\right) dv^2 + 2dv dr + r^2 d\Omega_2^2 \quad (6.8)$$

This is the Schwarzschild black hole in *ingoing Eddington-Finkelstein coordinates*. We see that the dr^2 terms have now disappeared, and so there is no singularity in the metric at $r = 2GM$. However, the dv^2 term vanishes at $r = 2GM$ and, moreover, flips sign for $r < 2GM$. You might worry that this means that the coordinates still go bad there, or even that the signature of the metric changes as we cross the horizon. To allay such worries, we need only compute the determinant of the metric

$$\det(g) = \det \begin{pmatrix} -(1 - \frac{2GM}{r}) & 1 & 0 & 0 \\ 1 & 0 & 0 & 0 \\ 0 & 0 & r^2 & 0 \\ 0 & 0 & 0 & r^2 \sin^2 \theta \end{pmatrix} = -r^4 \sin^2 \theta$$

We see that the $dv dr$ cross-term stops the metric becoming degenerate at the horizon and the signature remains Lorentzian for all values of r . (The metric is still degenerate at the $\theta = 0, \pi$ but these are simply the poles of the \mathbf{S}^2 and we know how to deal with that.)

This, then, is the advantage of the ingoing Eddington-Finkelstein coordinates: the r coordinate can be continued past the horizon, all the way down to the singularity at $r = 0$.

The original Schwarchild metric (6.1) was time independent. Mathematically, this follows from the statement that the metric exhibits a timelike Killing vector $K = \partial_t$. This Killing vector also exists in the Eddington-Finkelstein extension, where it is now $K = \partial_v$. The novelty is that this Killing vector is no longer everywhere timelike. Instead, it remains timelike outside the horizon where $g_{vv} < 0$, but becomes spacelike inside the horizon where $g_{vv} > 0$. In other words, the full black hole geometry is not time independent! We'll learn more about this feature as we progress.

The Finkelstein Diagram

To build further intuition for the geometry, we can look at the behaviour of light rays coming out of the black hole. These follow paths given by

$$u = t - r_\star = \text{constant}$$

Eliminating t , in preference of the null coordinate $v = t + r_\star$, outgoing null geodesics satisfy $v = 2r_\star + \text{constant}$. The solutions to this equation have a different nature depending on whether we are outside or inside the horizon. For $r > 2GM$, we can use the original definition (6.7) of the tortoise coordinate r_\star to get

$$v = 2r + 4GM \log \left(\frac{r - 2GM}{2GM} \right) + \text{constant}$$

Clearly the log term goes bad for $r < 2GM$. However, it is straightforward to write down a tortoise coordinate that obeys (6.6) on either side of the horizon: we simply need to take the modulus of the argument

$$r_\star = r + 2GM \log \left| \frac{r - 2GM}{2GM} \right|$$

This means that r_\star is multi-valued: it sits in the range $r_\star \in (-\infty, +\infty)$ outside the horizon, and in the range $r_\star \in (-\infty, 0)$ inside the horizon, with the singularity at $r_\star = 0$. Outgoing geodesics inside the horizon then obey

$$v = 2r + 4GM \log \left(\frac{2GM - r}{2GM} \right) + \text{constant} \tag{6.9}$$

It remains to find the outgoing null geodesic at the horizon $r = 2GM$. Here the dv^2 term in the metric (6.8) vanishes, and one can check that the surface $r = 2GM$ is itself a null geodesic. This agrees with our expectation from Section 6.1.2 where we saw that the horizon is a null surface.

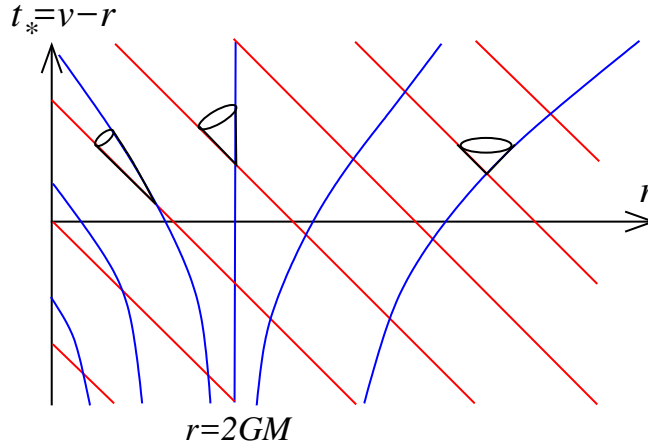


Figure 44: The Finkelstein diagram in ingoing coordinates. Ingoing null geodesics are shown in red, outgoing in blue. Inside the horizon at $r = 2GM$, outgoing geodesics do not go out.

We can capture this information in a *Finkelstein diagram*. This is designed so that ingoing null rays travel at 45 degrees. This is simple to do if we label the coordinates of the diagram by t and r_* . However, as we’ve seen, r_* isn’t single valued everywhere in the black hole. For this reason, we will label the spatial coordinate by the original r . We then define a new temporal coordinate t_* by the requirement

$$v = t + r_* = t_* + r$$

So ingoing null rays travel at 45 degrees in the (t_*, r) plane, where $t_* = v - r$. These are shown as the red lines in Figure 44. Meanwhile, the outgoing null geodesics are shown in blue. Now we can clearly see how the behaviour changes depending on whether the geodesics are inside or outside the horizon. The outgoing geodesics that sit outside the horizon do what their name suggests: they move out. In particular, as $t \rightarrow \infty$ (so $t_* \rightarrow \infty$), the geodesics escape to $r \rightarrow \infty$.

The outgoing geodesics that sit inside the horizon are not so lucky. Now as t increases, the geodesics described by (6.9) don’t go “out” at all: instead the “outgoing” light rays move inexorably towards the curvature singularity at $r = 0$. Each of them hits the singularity at some finite t_* .

Bounding these two regions are the null geodesics which simply run along the horizon $r = 2GM$: this is the vertical blue line in the figure.

We can also draw light-cones on the Finkelstein diagram. These are the regions bounded by the ingoing and outgoing, future-pointing null geodesics, as shown in the figure. Any massive particle must follow a timelike path, and hence its trajectory must sit within these lightcones. We see immediately one of the key features of black holes: if you venture into past the horizon, you're not getting back out again. This is forbidden by the causal structure of the spacetime. The term *black hole* really refers to the region $r < 2GM$ inside the horizon. Any observer who remains outside the horizon can know nothing about what's happening inside.

We can also use the Finkelstein diagram to tell us what an observer will see if they push their friend into a black hole. The hapless companion sails through the horizon, quite possibly without realising anything is wrong. However, any light signals that are sent back take longer and longer to reach an observer sitting at some fixed radial value $r > 2GM$. This means that the actions of the in-falling friend become increasingly slowed down as they approach the horizon. In this way, the observer/villain sitting outside continues to see their friend forever, but knows nothing of their action after they cross the horizon. Furthermore, since the light is now emerging from a deeper and deeper gravitational well, it will appear increasingly redshifted to the outside observer.

Outgoing Eddington-Finkelstein Coordinates

There is a different extension of the exterior of the Schwarzschild black hole, in which we replace the time coordinate t with the null coordinate

$$u = t - r_*$$

Recall the surfaces of constant u correspond to outgoing, radial, null geodesics.

As before, it is straightforward to make this change of variable. We have $t = u + r_*$, so

$$dt = du + dr_* = du + \left(1 - \frac{2GM}{r}\right)^{-1} dr$$

Making this substitution in the Schwarzschild metric (6.1), we now find the metric

$$ds^2 = - \left(1 - \frac{2GM}{r}\right) du^2 - 2du dr + r^2 d\Omega_2^2 \quad (6.10)$$

This is the Schwarzschild solution in *outgoing Eddington-Finkelstein coordinates*. The only difference with the ingoing coordinates (6.8) is the sign of the cross-term. However, as we now explain, this seemingly trivial difference greatly changes the interpretation of the metric.

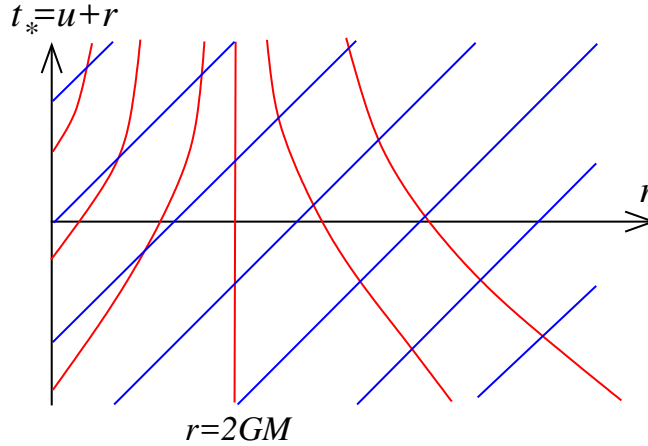


Figure 45: The Finkelstein diagram in outgoing coordinates. Ingoing null geodesics are shown in red, outgoing in blue. Inside the horizon at $r = 2GM$, ingoing geodesics do not go in.

Once again, the metric is smooth (and non-degenerate) at the horizon so we can happily continue the metric down to the singularity at $r = 0$. However, the region $r < 2GM$ now describes a different part of spacetime from the analogous region in ingoing Eddington-Finkelstein coordinates!

To see this, we can again look at the ingoing and outgoing geodesics, as seen in the Finkelstein diagram in Figure 45. This time, we pick coordinates so that the outgoing geodesics travel at 45 degrees. This means that we take r and $t_* = u + r$. The outgoing geodesics are drawn in red as before. But this time we see that they do what their name suggests: they go always go out, regardless of whether they start life behind the horizon.

This time, it is the ingoing null geodesics that have the interesting property. Those that start life outside are unable to reach the singularity. Instead, they pile up at the horizon. Those that start life behind the horizon have an even stranger property: the ingoing geodesics do not go in. Instead they too move towards the horizon, again unable to cross it.

We can also ask what becomes of massive particles that sit inside the horizon. As before, their trajectories must lie within future-pointing light cones. We see that they cannot linger inside the horizon for long. The causal structure of the spacetime ultimately ejects them into the region outside the horizon.

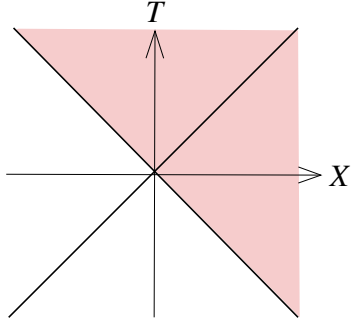


Figure 46: Ingoing coordinates cover this part of Rindler space.

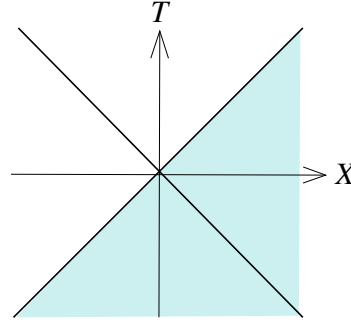


Figure 47: Outgoing coordinates cover this part.

This is clearly very different physics from a black hole. Instead, the solution (6.10) is that of a *white hole*, an object which expels any matter inside. This is the time reversal of a black hole, a fact which can be traced to the relative minus sign between the two metrics (6.8) and (6.10). This time reversal is also manifest in the diagrams: turn the white hole of Figure 45 upside down and you get the black hole of Figure 44.

White holes are perfectly acceptable solutions to the Einstein equations. Indeed, given the existence of black holes from which nothing can escape, the time reversal invariance of the Einstein equations tells us that there had to be a corresponding solution which nothing can enter. Nonetheless, white holes are not physically relevant since, in contrast to black holes, one cannot form them from collapsing matter.

6.1.4 Kruskal Spacetime

It may be somewhat surprising to learn that we can extend the $r \in (2GM, \infty)$ coordinate of the Schwarzschild solution in two different ways, so what we gain — the region parameterised by $r \in (0, 2GM]$ — corresponds to two different parts of spacetime! We can gain some intuition for this by returning to the near horizon limit of Rindler space. The region outside the black hole, covered by the Schwarzschild metric, corresponds to the right-hand quadrant of Rindler space. The ingoing Eddington-Finkelstein coordinates extend this to the upper quadrant, while the outgoing Eddington-Finkelstein coordinates extend it to the lower quadrant, as shown in the figures above. The purpose of this section is to understand this better. We will achieve this by introducing coordinates which cover the entire spacetime, including both black and white holes.

It is simple to write the Schwarzschild metric using both null coordinates $v = t + r_*$ and $u = t - r_*$. It becomes

$$ds^2 = - \left(1 - \frac{2GM}{r} \right) du dv + r^2 d\Omega_2^2 \quad (6.11)$$

where we should now view r^2 as a function $r^2(u - v)$. In these coordinates, the metric is degenerate at $r = 2GM$ so we need to do somewhat better. This can be achieved by introducing the *Kruskal-Szekeres coordinates*,

$$U = -\exp\left(-\frac{u}{4GM}\right) \quad \text{and} \quad V = \exp\left(\frac{v}{4GM}\right) \quad (6.12)$$

Both U and V are null coordinates. As defined above, the exterior of the Schwarzschild black hole is parameterised by $U < 0$ and $V > 0$. They have the further property that, outside the horizon,

$$UV = -\exp\left(\frac{r_\star}{2GM}\right) = \frac{2GM - r}{2GM} \exp\left(\frac{r}{2GM}\right) \quad (6.13)$$

where, in the second equality, we've used the definition (6.7) of the tortoise coordinate. Similarly,

$$\frac{U}{V} = -\exp\left(-\frac{t}{2GM}\right) \quad (6.14)$$

A quick calculation shows that the metric (6.11) becomes

$$ds^2 = -\frac{32(GM)^3}{r} e^{-r/2GM} dU dV + r^2 d\Omega_2^2 \quad (6.15)$$

where $r(U, V)$ is the function defined by inverting (6.13).

The original Schwarzschild metric covers only the region of spacetime with $U < 0$ and $V > 0$. But now we can happily extend the range to $U, V \in \mathbf{R}$, with the function $r(U, V)$ again defined by (6.13). We see that now nothing bad happens at $r = 2GM$: the metric is smooth and non-degenerate.

Analytic Extensions

Given the amount of games we've played above, jumping between different coordinate systems, one may wonder if there are further games in which the Kruskal spacetime can be extended yet further. This turns out not to be the case: the Kruskal spacetime is the maximal extension of the Schwarzschild solution.

Here is the way to check whether a given spacetime can be extended: look at all geodesics and see where they end up. If you can follow geodesics for infinite affine parameter, then they escape to infinity. If, on the other hand, geodesics come to an end at some finite affine parameter then something is going on: either they run into a genuine singularity, or they run into a coordinate singularity. In the former case there's nothing you can do about it. In the latter case, you can extend the spacetime as we have above. You have the maximally extended spacetime when any geodesics that come to an abrupt halt do so at genuine singularities.

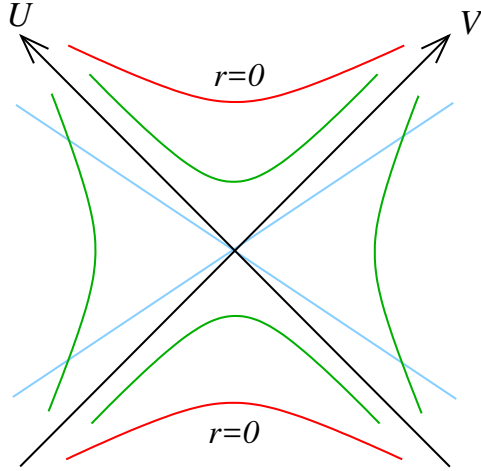


Figure 48: The Kruskal diagram for the Schwarzschild black hole. The U and V axes are the horizons at $r = 2GM$ and the red lines are the singularities at $r = 0$. Also shown are lines of constant r in green, and lines of constant t in blue.

There is something a little magical about the extension process. We start off with a solution to the Einstein equations in some region of spacetime. Yet this is sufficient to determine the metric throughout the entire, extended spacetime. In particular, once we've extended, we don't have to solve the Einstein equations from scratch. This magic follows from the fact that the metric components are real, analytic functions. This means that knowledge of the metric in any open set is sufficient to determine it everywhere.

The Kruskal Diagram

We can see what becomes of the horizon in the new coordinates by using (6.13). We have

$$r = 2GM \quad \Rightarrow \quad U = 0 \text{ or } V = 0$$

This tells us that the horizon is not one null surface, but two null surfaces, intersecting at the point $U = V = 0$. This agrees with what we learned from taking the near horizon limit where we encountered Rindler space. The null surface $U = 0$ is the horizon of the black hole; it is called the *future horizon*. The null surface $V = 0$ is the horizon of the white hole; it is the *past horizon*.

We can also see what becomes of the singularity. This now sits at

$$r = 0 \quad \Rightarrow \quad UV = 1$$

The hyperbola $UV = 1$ has two disconnected components. One of these, with $U, V > 0$, corresponds to the singularity of the black hole. The other, with $U, V < 0$ corresponds to the singularity of the white hole.

These facts can be depicted on a *Kruskal diagram*, shown in Figure 48. The U and V axes are drawn at 45 degrees, reflecting the fact that they are null lines. These are the two horizons. In this diagram, the vertical direction can be viewed as the time $T = \frac{1}{2}(V + U)$ while the horizontal spatial direction is $X = \frac{1}{2}(V - U)$. The singularities $UV = 1$ are drawn in red. This diagram makes it clear how the black hole and white hole cohabit in the same spacetime.

The diagram also shows lines of constant r , drawn in green, and lines of constant t drawn in blue. From (6.13), we see that lines of constant r are given by $UV = \text{constant}$. Meanwhile, from (6.14), lines of constant t are linear, given by $U/V = \text{constant}$.

The diagram contains some important lessons. You might have naively thought that the singularity of the black hole was a point that traced a timelike worldline, similar to any other particle. The diagram makes it clear that this is not the case: instead, the singularity is *spacelike*. Once you pass through the horizon, the singularity isn't something that sits to your left or to your right: it is something that lies in your future. This makes it clear why you cannot avoid the singularity when inside a black hole. It is your fate. Similarly, the singularity of the white hole lies in the past. It is similar to the singularity of the Big Bang.

We can frame this in terms of the Killing vector of the Schwarzschild solution $K = \partial_t$. This is timelike outside the horizon and, indeed, gives rise to the conserved energy of geodesics outside the black hole that we met in Section 1.3. In the Kruskal coordinates, we can use (6.12) to find

$$K = \frac{\partial}{\partial t} = \frac{\partial V}{\partial t} \frac{\partial}{\partial V} + \frac{\partial U}{\partial t} \frac{\partial}{\partial U} = \frac{1}{4GM} \left(V \frac{\partial}{\partial V} - U \frac{\partial}{\partial U} \right)$$

Evaluating the norm of this Killing vector in the Kruskal metric (6.15), we have

$$g_{\mu\nu} K^\mu K^\nu = - \left(1 - \frac{2GM}{r} \right)$$

We see that outside the horizon, the Killing vector is timelike as expected. But inside the horizon, with $r < 2GM$, the Killing vector is spacelike. (We saw similar behaviour when discussing the isometries of de Sitter space in Section 4.3.1.) When we say that a spacetime is time independent, we mean that there exists a timelike Killing vector. We learn that the full black hole spacetime is *not* time independent. But this only becomes apparent once you cross the horizon.

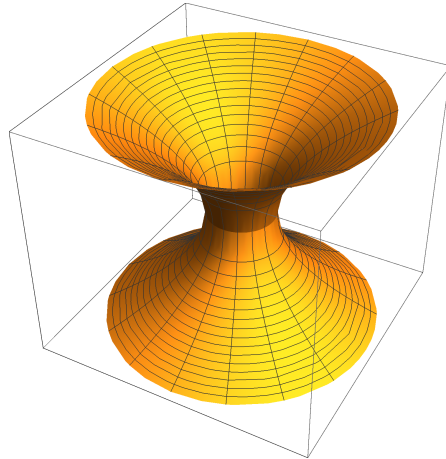


Figure 49: The Einstein-Rosen Bridge

A hint of this, albeit one that cannot be trusted, can be seen in the original Schwarzschild solution (6.1). If we were to take this at face value for $0 < r < 2GM$, we see that the change of sign in $(1 - 2GM/r)$ means that the vector ∂_t becomes spacelike and the vector ∂_r timelike. This again suggests that the singularity lies in the future or the past. All the hard work in changing coordinates above shows that this naive result is, in fact, true.

The Einstein-Rosen Bridge

We now understand three of the four quadrants of the Kruskal diagram. The right-hand quadrant is the exterior of the black hole, which is the spacetime covered by the original Schwarzschild coordinates. The upper quadrant is the interior of the black hole and the lower quadrant is the interior of the white hole. This leaves the left-hand quadrant. This is a surprise: it is another copy of the exterior of the black hole, now covered by $U > 0$ and $V < 0$. To see this, we can write

$$U = + \exp\left(-\frac{u}{4GM}\right) \quad \text{and} \quad V = - \exp\left(\frac{v}{4GM}\right)$$

Going back through the various coordinate transformations then shows that the left-hand quadrant is again described by the Schwarzschild metric.

What are we to make of this? Our final spacetime contains two asymptotically flat regions joined together by a black hole! That sounds rather wild. Note that it's not possible for an observer in one region to send a signal to an observer in another because the causal structure of the spacetime does not allow this. Nonetheless, we could ask: what is the spatial geometry that connects the two regions?

To elucidate this spatial geometry, we look at the $t = 0$ slice of Kruskal spacetime. This is a straight, horizontal line passing through $U = V = 0$. If we return to our original Schwarzschild metric then, at $t = 0$, the spatial geometry is given by

$$ds^2 = \left(1 - \frac{2GM}{r}\right)^{-1} dr^2 + r^2(d\theta^2 + \sin^2\theta d\phi^2) \quad (6.16)$$

which is valid for $r > 2GM$. This describes the geometry in the right-hand quadrant. There is another copy of the same geometry in the left-hand quadrant. We then glue these together at $r = 2GM$, to give a wormhole-like geometry as shown in Figure 49. This wormhole is called the *Einstein-Rosen bridge*. It's not a wormhole that you can travel through because the paths are spacelike, not timelike.

It's possible to write down a metric that includes both sides of the wormhole. To do this we introduce a new radial coordinate ρ , defined by

$$r = \rho \left(1 + \frac{GM}{2\rho}\right)^2 = \rho + GM + \frac{G^2M^2}{4\rho} \quad (6.17)$$

This is plotted in the figure. It has the property that there are two values of ρ for each value of $r > 2GM$. At the horizon, $r = 2GM$, there is just a single value: $\rho = GM/2$. The idea is that $\rho > GM/2$ parameterises one side of the wormhole while $\rho < GM/2$ parameterises the other. Substituting r for ρ in (6.16) gives the metric

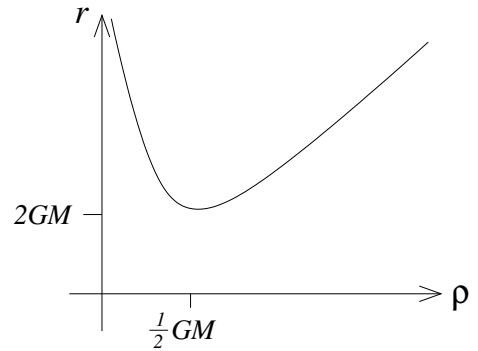


Figure 50:

$$ds^2 = \left(1 + \frac{GM}{2\rho}\right)^4 [d\rho^2 + \rho^2(d\theta^2 + \sin^2\theta d\phi^2)] \quad (6.18)$$

(To show this, it's useful to first show that $(1 - 2GM/r) = (1 - GM/2\rho)^2(1 + 2GM/\rho)^{-2}$.) Clearly this metric looks like flat \mathbf{R}^3 as $\rho \rightarrow \infty$ since we can drop the overall factor. Less obviously, it also looks like flat \mathbf{R}^3 as $\rho \rightarrow 0$. To see this, note that there is a symmetry of (6.17) under $\rho \rightarrow G^2M^2/4\rho$, which swaps the two asymptotic spacetimes, leaving the meeting point at $\rho = GM/2$ invariant. In this way, the metric (6.18) describes the two-sided Einstein-Rosen bridge shown in Figure 49.

The radius of the \mathbf{S}^2 is $2GM$ in the middle of the wormhole at $\rho = GM/2$, and then grows as we move away in either direction. This middle point is where the two horizons $U = 0$ and $V = 0$ meet. In fancy language, it is called the *bifurcation sphere*.

ER = EPR?

Although there is no way that an observer in the left-most quadrant can signal to an observer in the right-most quadrant, there is one way in which they can communicate: both need to be brave and jump into the black hole. Then they can both meet behind the horizons and share their stories.

This sounds like a rather wild idea! Is it physically meaningful? After all, the white hole that sits in the bottom quadrant is thought to have no physical manifestation. Similarly, it seems likely that for generic black holes the other universe that appeared in the left quadrant of the Kruskal diagram is also a mathematical artefact. Nonetheless, there is one rather speculative proposal in which such communication behind the horizon may be possible.

First, we can dispel the idea that the two asymptotic regimes necessarily correspond to different universes. One could patch together the asymptotic parts of the two Minkowski spaces so that the Kruskal diagram gives an approximate description of two, far separated black holes in the same universe. This would be an approximate solution to the field equations since, no matter how far, the two black holes would attract.

Viewed in this way, the Kruskal diagram suggests that two observers, potentially living billions of light years apart, could jump into these far flung black holes and meet behind the horizon. They could then have a nice chat before their inevitable demise in the singularity. Is this outlandish idea possible? And, if so, which pairs of black holes in the universe are connected in this way?

A proposal, emerging from ideas in quantum gravity, suggests that two black holes are connected in this way if they have some measure of quantum entanglement. This proposal goes by the cute name of ER = EPR, with ER denoting the Einstein-Rosen bridge characterising a geometric connection, and EPR denoting the entanglement of the Einstein-Podolsky-Rosen paradox. (More details of entanglement can be found in the lectures on [Topics in Quantum Mechanics](#).) It is far from clear that the ER=EPR proposal is correct, but it is certainly a tantalising idea.

The Penrose Diagram

As we explained in Section 4.4.2, the best way to exhibit the causal structure of a spacetime is to draw the Penrose diagram. For the black hole, this is very similar to the Kruskal diagram: we simply straighten out a few lines.

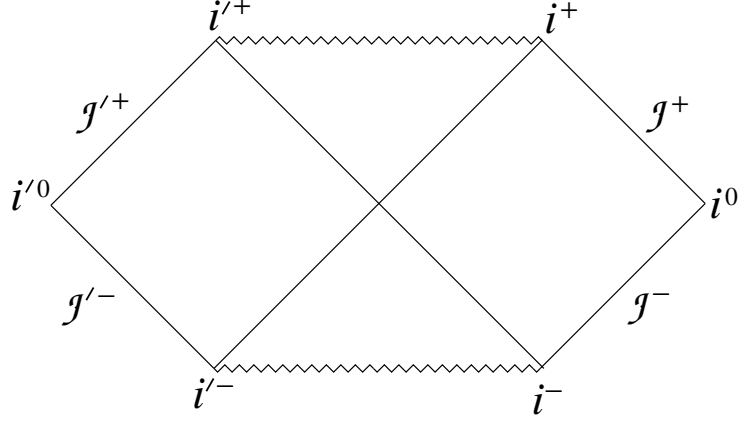


Figure 51: The Penrose diagram for the Schwarzschild black hole. The right quadrant describes the asymptotically flat region external to the black hole. The upper quadrant is the black hole and the lower quadrant a white hole, each with spacelike singularities shown as jagged lines. The left quadrant is another asymptotically flat region spacetime.

The first step is to introduce new coordinates which cover the entire space in a finite range. We use the same kind of transformation that we saw in many examples in Section 4.4.2, namely

$$U = \tan \tilde{U} \quad \text{and} \quad V = \tan \tilde{V}$$

The new coordinates have finite range $\tilde{U}, \tilde{V} \in (-\pi/2, +\pi/2)$. The Kruskal metric (6.15) is then

$$ds^2 = \frac{1}{\cos^2 \tilde{U} \cos^2 \tilde{V}} \left[-\frac{32(GM)^3}{r} e^{-r/2GM} d\tilde{U} d\tilde{V} + r^2 \cos^2 \tilde{U} \cos^2 \tilde{V} d\Omega_2^2 \right]$$

This metric is then conformal to the (slightly!) simpler metric

$$d\tilde{s}^2 = -\frac{32(GM)^3}{r} e^{-r/2GM} d\tilde{U} d\tilde{V} + r^2 \cos^2 \tilde{U} \cos^2 \tilde{V} d\Omega_2^2$$

However, we must remember the singularity. This sits at $r = 0$ or $UV = 1$. In the finite range coordinates this means

$$\tan \tilde{U} \tan \tilde{V} = 1 \quad \Rightarrow \quad \sin \tilde{U} \sin \tilde{V} - \cos \tilde{U} \cos \tilde{V} = 0 \quad \Rightarrow \quad \cos(\tilde{U} + \tilde{V}) = 0$$

In other words, the singularity sits at $\tilde{U} + \tilde{V} = \pm\pi/2$. These are straight, horizontal lines in the Penrose diagram.

In the absence of the singularities, \tilde{U} and \tilde{V} would have a diamond-shaped Penrose diagram, like that of 2d Minkowski space. The presence of the singularities mean that the top and bottom are chopped off, resulting in the Penrose diagram for the Schwarzschild black hole shown in Figure 51. This diagram contains the same information as the Kruskal diagram that we saw previously.

The Penrose diagram allows us to give a more rigorous definition of a black hole. Here we'll eschew any pretense at rigour, but give a flavour of the definition. We restrict attention to asymptotically flat spacetimes, meaning that far away they look like Minkowski space. This means, in particular, the asymptotic region includes both two null infinities, \mathcal{I}^+ and \mathcal{I}^- . (We will further require that the metric looks like Minkowski space near \mathcal{I}^\pm although we'll be sloppy about specifying what we mean by this.) The black hole region is then defined to be the set of points that cannot send a signal to \mathcal{I}^+ . The boundary of the black hole region is the future event horizon, \mathcal{H}^+ . Equivalently, the future event horizon \mathcal{H}^+ is the boundary of the causal past of \mathcal{I}^+ .

In the Penrose diagram of Figure 51, the black hole region associated to \mathcal{I}^+ is the upper quadrant and the left quadrant. The black hole associated to \mathcal{I}'^+ is the upper quadrant and the right quadrant.

Importantly, to define a black hole you need to know the whole of the spacetime: you run lightrays backwards from \mathcal{I}^+ and the boundary of these light rays defines the event horizon. There is no definition of the black hole region that refers only to a spacelike slice Σ at some moment in (a suitably defined) time. This means that an observer can't really know if they're inside a black hole unless they know the entire future evolution of the spacetime.

Relatedly, we can also define the white hole region to be that part of spacetime that cannot receive signals from \mathcal{I}^- . The boundary of the white hole region is the past event horizon, \mathcal{H}^- .

6.1.5 Forming a Black Hole: Weak Cosmic Censorship

The Kruskal spacetime that we have discussed so far is unphysical in a number of ways. In reality, black holes do not emerge from white holes! Instead, they are formed by collapsing stars. The causal structure of such realistic black holes looks rather different from the Penrose diagram of figure 51.

We could try to write down solutions corresponding to collapsing stars. In fact, this is not too difficult. However, our main interest here is to understand the causal structure of the spacetime and we can do this by patching together things that we already know.

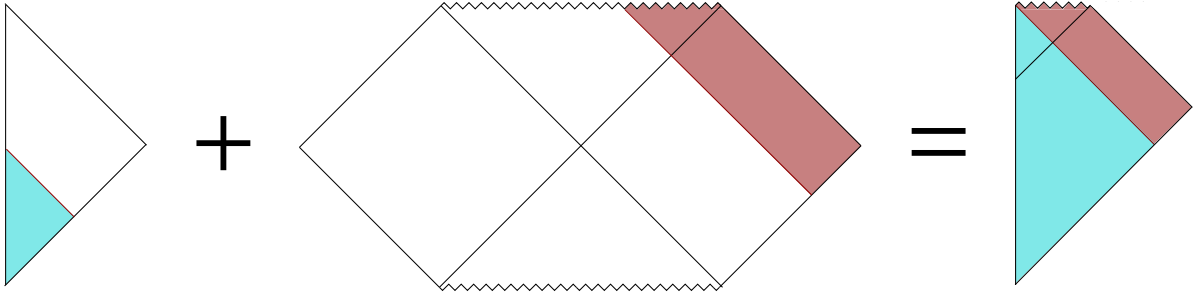


Figure 52: Joining two Penrose diagrams

Things are conceptually most straightforward if we consider the unrealistic situation of the spherically symmetric collapse of a shell of matter. Inside the shell, spacetime is flat. Outside the shell, spacetime is described by the Schwarzschild geometry (6.1). Birkhoff’s theorem tells us that this latter statement remains true even for time-dependent collapsing shells. If we further make the (again, unrealistic) assumption that the shell is travelling at the speed of light, then we can glue together the Penrose diagrams for Minkowski spacetime and the black hole spacetime, as shown in Figure 52. This gives the Penrose diagram for a collapsing black hole.

Although we made a number of assumptions in the above paragraph, the Penrose diagram that we derived also describes the spherical collapse of realistic stars. In this case, the surface of the star follows a timelike trajectory, as shown in the figure to the right. The unphysical parts of the Kruskal diagram have now disappeared: there is no white hole and no mirror universe.

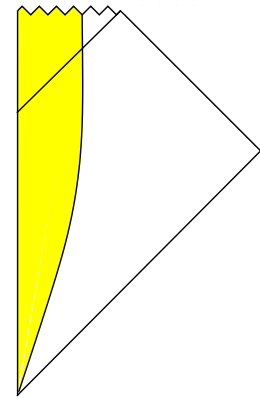


Figure 53:

Cosmic Censorship

One important feature of the black hole remains: the singularity is shrouded behind the horizon. This means that the effects of the singularity cannot be felt by an asymptotic observer. We can ask: is this always the case? Or could we end up with a singularity which is not hidden by a horizon. Such singularities are called *naked singularities*

Naked singularities are commonplace in solutions to Einstein’s equations. The white hole of the full Kruskal spacetime provides one example; the Big Bang singularity provides another. Yet another is provided by the Schwarzschild metric. This solves the Einstein equations for all M , but is only physical for $M \geq 0$. With $M < 0$, we can



Figure 54: On the left: the Penrose diagram for a negative mass black hole. On the right: this kind of collapsing star scenario is forbidden by weak cosmic censorship.

write the Schwarzschild metric as

$$ds^2 = - \left(1 + \frac{2G|M|}{r} \right) dt^2 + \left(1 + \frac{2G|M|}{r} \right)^{-1} dr^2 + r^2(d\theta^2 + \sin^2 \theta d\phi^2)$$

Now there is no coordinate singularity at $r = 2G|M|$ and, correspondingly, no horizon. We can construct the Penrose diagram for this spacetime in the same way that we did for Minkowski space, now using null coordinates $u = t - r$ and $v = t + r$. The final result is exactly the same as Minkowski space, with one difference: there is a curvature singularity at $r = 0$. The Penrose diagram is shown in the left-hand figure above. The singularity of the $M < 0$ black hole is not shielded behind a horizon. It is a naked singularity whose effects can be observed from \mathcal{I}^+ .

Despite the ubiquity of naked singularities in solutions to the Einstein equations, there is a general belief that they are unphysical. (The Big Bang singularity is an important exception to this and we will comment further on this case below.) A deep conjecture in general relativity, known as *weak cosmic censorship*, says that naked singularities cannot form. To phrase the cosmic censorship conjectures precisely, we would need to discuss the initial value problem in general relativity. The initial conditions are specified on a spatial hypersurface and are subsequently evolved through the equations of motion. The *weak cosmic censorship conjecture* states the following

The Weak Cosmic Censorship Conjecture: Given matter which obeys the dominant energy condition (described in Section 4.5.7), generic, smooth initial conditions for both the metric and matter fields in an asymptotically flat spacetime will not evolve to form naked singularities.

There are a whole bunch of caveats in this statement. Each of them is important. It turns out that it is possible to construct finely tuned initial conditions (of measure zero in the space of all initial conditions) that result in naked singularities; hence the need for the word “generic”. It turns out that it is also possible to violate weak cosmic censorship in asymptotically AdS spacetimes. Finally, the naked singularity of the $M < 0$ black hole gives some intuition for why we need the energy of the matter fields to obey some positivity condition.

If weak cosmic censorship is true, then it rules out dynamical evolution such as that shown in right hand figure. In fact, this diagram is somewhat misleading. Once the singularity forms, we can no longer evolve the fields beyond the light-ray shown as a dotted red line in the figure. This means that, strictly speaking, the dynamical evolution stops at the red line and can’t be extended beyond. A more precise statement of the weak cosmic censorship conjecture hinges on this idea and, in particular, the statement that \mathcal{I}^+ doesn’t just come to an abrupt end.

There is no proof of weak cosmic censorship: indeed, it is arguably the biggest open question in mathematical relativity. Nonetheless, a wealth of numerical and circumstantial evidence supports the claim.

What should we make of cosmic censorship? At a practical level, it is a boon for those who work on numerical relativity, since it means that the simulations can proceed without worrying about how to cope with singularities. But for the rest of us, cosmic censorship is rather disappointing. This is because singularities – or, more generally, regions of high curvature – are where we expect quantum gravity effects to become important. Cosmic censorship means that it is unlikely we will have observational access to such behaviour. It is both striking and surprising that classical gravity finds a way to protect us from the ravages of quantum gravity.

There is one naked singularity that does appear to be physical: this is the Big Bang singularity. Since this lives in the far past, it certainly doesn’t violate the cosmic censorship conjecture. It’s tempting to think that we may ultimately be able to see the effects of quantum gravity here. Sadly, this hope too seems to be quashed, with inflation washing away the details of the very early universe. Quantum gravity is, it seems, a difficult observational science.

6.1.6 Black Holes in (Anti) de Sitter

Throughout this section we have focussed on black holes in asymptotically Minkowski spacetime. It is not hard to find solutions corresponding to Schwarzschild black holes

in de Sitter and anti-de Sitter spacetimes, solving the Einstein equations

$$R_{\mu\nu} = \Lambda g_{\mu\nu}$$

We have already done the hard work. We take the ansatz

$$ds^2 = -f(r)^2 dt^2 + f(r)^{-2} dr^2 + r^2(d\theta^2 + \sin^2 \theta d\phi^2)$$

We saw in Section 4.2 that this obeys the Einstein equations provided that

$$f'' + \frac{2f'}{r} + \frac{f'^2}{f} = -\frac{\Lambda}{f} \quad \text{and} \quad 1 - 2ff'r - f^2 = \Lambda r^2$$

These equations have the solution

$$f^2 = 1 - \frac{2GM}{r} \mp \frac{r^2}{R^2}$$

with $R^2 = 3/|\Lambda|$. Here the minus sign solves the equation with $\Lambda > 0$ and the plus sign with $\Lambda < 0$. They correspond to black holes in de Sitter and anti-de Sitter spacetimes respectively. To see that this is the right interpretation, consider the metric with $2MG \ll R^2$, so that the Schwarzschild radius is much less than the curvature of spacetime. Then, for $r \ll R$, the metric looks like that of a Schwarzschild black hole in flat space. We will not have anything more to say about these solutions in these lectures.

6.2 Charged Black Holes

In this section, we describe a solution to the Einstein-Maxwell equation corresponding to a black hole carrying electric or magnetic charge.

Black holes with large amounts of electric charge do not arise in Nature. (Such black holes would attract the opposite charge and neutralise.) Nonetheless, there are a number of theoretical reasons for studying these black holes. In particular, charged black holes exhibit a rather different causal structure from the Schwarzschild solution and, for our purposes, this will provide a warm-up for the rotating black holes that we will study in Section 6.3. Moving beyond these lectures, it turns out that charged black holes provide a laboratory in which we can address certain questions about the quantum make-up of black holes.

6.2.1 The Reissner-Nordström Solution

Charged black holes arise as a solution to Einstein-Maxwell theory, with action

$$S = \int d^4x \sqrt{-g} \left[\frac{1}{16\pi G} R - \frac{1}{4} F^{\mu\nu} F_{\mu\nu} \right] \quad (6.19)$$

The equations of motion are the Maxwell equation

$$\nabla^\mu F_{\mu\nu} = 0$$

together with the Einstein-Maxwell equation

$$R_{\mu\nu} - \frac{1}{2} R g_{\mu\nu} = 8\pi G \left(F_\mu{}^\rho F_{\nu\rho} - \frac{1}{4} g_{\mu\nu} F^{\rho\sigma} F_{\rho\sigma} \right)$$

where the right-hand side is the Maxwell stress-energy tensor that we calculated in (4.52).

These equations of motion admit a spherically symmetric solution with gauge field

$$A = -\frac{Q_e}{4\pi r} dt - \frac{Q_m}{4\pi} \cos\theta d\phi$$

The metric takes the familiar spherically symmetric form

$$ds^2 = -f(r)^2 dt^2 + f(r)^{-2} dr^2 + r^2 d\Omega_2^2$$

where, this time,

$$f(r)^2 = 1 - \frac{2GM}{r} + \frac{e^2}{r^2} \quad \text{with} \quad e^2 = \frac{G}{4\pi} (Q_e^2 + Q_m^2)$$

This is the *Reissner-Nordström solution*, discovered over a period of years from 1916 to 1921.

An analog of Birkhoff's theorem says that the Reissner-Nordström solution is almost the unique spherically symmetric solution of the Einstein-Maxwell equations. There is one exception: there is a solution with geometry $\text{AdS}_2 \times \mathbf{S}^2$, threaded with electric flux; we'll see how this emerges a special limit of the Reissner-Nordström solution in Section 6.2.5.

The dt term in the gauge field describes a radial electric field. Meanwhile, the $d\phi$ term is the gauge field for a magnetic monopole; it is only rotationally invariant up to a gauge transformation. (See, for example, the lectures on [Gauge Theory](#) for more discussion.) Both of these charges can be measured asymptotically as explained in 3.2.5. One can check that

$$Q_e = \int_{\mathbf{S}^2} \star F \quad \text{and} \quad Q_m = \int_{\mathbf{S}^2} F$$

The solution has non-vanishing electric and magnetic charge, even though the theory (6.19) has no charge matter. The electric and magnetic charges can be viewed as lurking in the singularity.

To get some intuition for the Reissner-Nordström black hole, we write the metric factor as

$$f(r)^2 = \frac{1}{r^2}(r - r_+)(r - r_-)$$

Here the two roots are given by

$$r_{\pm} = GM \pm \sqrt{G^2M^2 - e^2} \tag{6.20}$$

In the limit where $e \rightarrow 0$, the smaller root merges with the singularity, $r_- \rightarrow 0$ while the larger root coincides with the Schwarzschild radius $r_+ \rightarrow 2GM$. The physical interpretation of the metric depends on the roots of this polynomial. We deal with these cases in turn.

6.2.2 Super-Extremal Black Holes

Super-extremal black holes have $|e| > GM$. This means that $f(r)^2$ has no zero, and so the metric has no horizon. This situation is analogous to the negative mass Schwarzschild solution. It has a naked singularity. It is unphysical.

If we take, for example, an electrically charged black hole, the super-extremal condition $e^2 > G^2M^2$ translates to the requirement that $Q_e^2/4\pi > GM^2$. But this ensures that the electromagnetic repulsion between two such black holes beats the gravitational attraction. For this reason, it is hard to see how such objects could form in the first place.

Of course, all charged sub-atomic particles are super-extremal in the sense that the electrical repulsion beats the gravitational attraction. There is no contradiction here: sub-atomic particles simply are not black holes! For example, a particle with mass m

has Compton wavelength $\lambda = \hbar/2\pi mc$. (For once we've put the factor of c back in this equation.) The requirement that the Compton wavelength is always larger than the Schwarzschild radius is

$$\frac{\hbar}{2\pi mc} > \frac{2Gm}{c^2} \quad \Rightarrow \quad m^2 < \frac{\hbar c}{4\pi G} = 2M_{\text{pl}}^2$$

This conclusion should not be surprising: it tells us that quantum effects are more important than gravitational effects for any sub-atomic particle that weighs less than the Planck mass, which itself is a whopping 10^{18}GeV . This is roughly the mass of a grain of sand.

6.2.3 Sub-Extremal Black Holes

Reissner-Nordström black holes with $|e| < GM$ are called sub-extremal. These are the physically relevant solutions.

There are now two roots, r_{\pm} , of the metric function $f(r)^2$. The Kretschmann scalar diverges at neither of these roots, suggesting that both are horizons. So charged black holes have two horizons: an outer one at r_+ and an inner one at r_- .

The presence of two roots changes the role played by the singularity. This is because the g_{rr} metric component flips sign twice so that r is again a spatial coordinate by the time we get to $r < r_-$. This suggests that $r = 0$ is now a timelike singularity, as opposed to the spacelike singularity that we saw in the Schwarzschild case. The purpose of this section is to understand these points in some detail.

We will follow the same path that we took to understand the Schwarzschild solution. We start by introducing a tortoise coordinate, analogous to (6.6), now defined by

$$dr_{\star}^2 = \frac{1}{f(r)^4} dr^2$$

The solution to this differential equation is

$$r_{\star} = r + \frac{1}{2\kappa_+} \log \left| \frac{r - r_+}{r_+} \right| + \frac{1}{2\kappa_-} \log \left| \frac{r - r_-}{r_-} \right| \quad (6.21)$$

with

$$\kappa_{\pm} = \frac{r_{\pm} - r_{\mp}}{2r_{\pm}^2}$$

We will see later that κ_{\pm} have the interpretation of the *surface gravity* on the two horizons.

The tortoise coordinate r_\star takes values in $r_\star \in (-\infty, +\infty)$ as $r \in (r_+, \infty)$. We introduce a pair of null coordinates, just as for the Schwarzschild black hole

$$v = t + r_\star \quad \text{and} \quad u = t - r_\star$$

Exchanging t in favour of the null coordinate v , we get the Reissner-Nordström black hole in ingoing Eddington-Finkelstein coordinates

$$ds^2 = -f(r)^2 dv^2 + 2dv dr + r^2 d\Omega_2^2 \quad (6.22)$$

This metric is smooth for all $r > 0$, and has a coordinate singularity at $r = 0$. This ensures that we can extend the Reissner-Nordström black hole to all $r > 0$. The same kind of arguments that we used for the Schwarzschild black hole again tell us that $r = r_+$ is a null surface, and no signal from $r < r_+$ can reach \mathcal{I}^+ . In other words, $r = r_+$ is a future event horizon.

Similarly, we could extend the Reissner-Nordström solution using outgoing Eddington-Finkelstein coordinates, to reveal a white hole region.

Kruskal Spacetime

We have still to understand the role played by the inner horizon at $r = r_-$ and, relatedly, the global structure of the spacetime. To make progress, we introduce two different kinds of Kruskal-like coordinates

$$U_\pm = -e^{-\kappa_\pm u} \quad \text{and} \quad V_\pm = \pm e^{\kappa_\pm v} \quad (6.23)$$

In the limit $e \rightarrow 0$, we have $\kappa_+ \rightarrow 4GM$ and the coordinates U_+ and V_+ coincide with the Kruskal-Szekeres coordinates (6.12).

To start, we work with the coordinates U_+ and V_+ . These null coordinates have the property that

$$U_+ V_+ = -e^{2\kappa_+ r_\star} = - \left(\frac{r - r_+}{r_+} \right) \left(\frac{r_-}{r - r_-} \right)^{r_-^2/r_+^2} e^{2\kappa_+ r} \quad (6.24)$$

The Reissner-Nordström metric is now,

$$\begin{aligned} ds^2 &= -f(r)^2 du dv + r^2 d\Omega_2^2 \\ &= -\frac{r_+ r_-}{\kappa_+^2 r^2} \left(\frac{r - r_-}{r_-} \right)^{1+r_-^2/r_+^2} e^{-2\kappa_+ r} dU_+ dV_+ + r^2 d\Omega_2^2 \end{aligned}$$

where, as usual, we should now view $r = r(U_+, V_+)$, this time using (6.24). The metric has started to get a little ugly, but the exact form won't bother us. More interesting is what the various regimes of U_+ and V_+ coordinates correspond to.

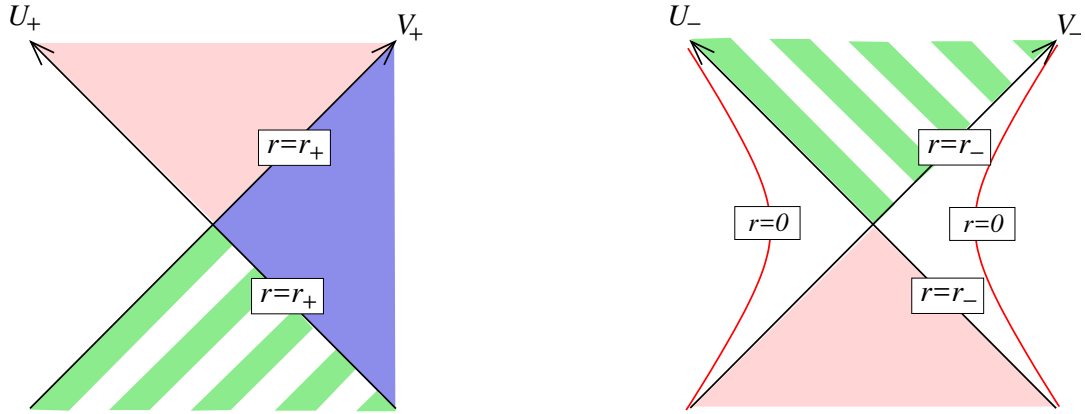


Figure 55:

The exterior of the Reissner-Nordström black hole is the region $r > r_+$. From (6.23) and (6.24), we see that this corresponds to $U_+ < 0$ and $V_+ > 0$. But, just as for the Schwarzschild-Kruskal spacetime, we can now extend the Kruskal coordinates to $U_+, V_+ \in \mathbf{R}$. This gives the now-familiar spacetime diagram, split into four quadrants depending on the sign of U_+ and V_+ . This is shown in the left-hand diagram of Figure 55; the region outside the horizon is the right-hand quadrant and is shaded blue; the region $r_- < r < r_+$ is the upper quadrant and is shaded pink.

At this point, however, the story diverges from that of Schwarzschild. This is because the Kruskal-type coordinates U_+ and V_+ do not extend down to the singularity at $r = 0$. Instead, from (6.24), we see that as $r \rightarrow r_-$, we have $U_+ V_+ \rightarrow \infty$. This means that the coordinates U_+ and V_+ only extend down to the inner horizon $r = r_-$.

There was no such obstacle in the Eddington-Finkelstein coordinates (6.22), which happily extended down to the singularity at $r = 0$. This means that the Kruskal coordinates U_+ and V_+ are not the final extension: we can do better.

This is where the other coordinates U_- and V_- in (6.23) come in. The regime between the horizons with $r_- < r < r_+$ (in ingoing Eddington-Finkelstein coordinates) corresponds to $U_-, V_- < 0$. We then have

$$U_- V_- = e^{2\kappa - r_*} = \left(\frac{r - r_-}{r_-} \right) \left(\frac{r_+}{r_+ - r} \right)^{r_+^2/r_-^2} e^{2\kappa - r}$$

These coordinates have the property that $U_- V_- \rightarrow \infty$ as $r \rightarrow r_+$ from below. In other words, they cover the region inside the black hole, but not outside. We can now

extend the U_- , V_- coordinates, as shown in the right-hand diagram of Figure 55, where the lower-most quadrant is shaded pink, to show that it should be identified with the upper-most quadrant of the first figure.

The U_- , V_- coordinates cover the singularity at $r = 0$. In fact, there are two such singularities, one in each of the left and right-quadrants as shown as red lines in the figure. Spacetime does not extend beyond the singularity. Importantly, and in contrast to the Schwarzschild black hole, the singularities are timelike. This is the kind of singularity that you might have imagined black holes to have: it is like the worldline of a particle. However, this means that there is nothing inevitable about the singularity of the Reissner-Nordström black hole: there exist timelike worldlines that a test particle could follow that miss the singularity completely.

Such fortunate worldliners will ultimately end up in the upper-most quadrant of the right-hand diagram of Figure 55, where $U_-, V_- > 0$. This is a new, unanticipated part of spacetime. One finds that geodesics hit the boundary of this region at a finite value of the affine parameter. This means that our spacetime must be extended yet further! In fact, the upper-most region of the right-hand diagram is isomorphic to the lower-most region of the left-hand diagram. These regions are shaded in the same colour, but with different stripes to show that the metrics are isomorphic, but they should not be identified. (Doing so would lead to a closed timelike curve.) Instead, we introduce yet a third set of coordinates, U'_+ and V'_+ . This gives rise to a new part of spacetime, isomorphic to the left-hand diagram. The whole procedure then repeats ad infinitum.

The Kruskal diagrams can be patched together to give the Penrose diagram for the Reissner-Nordström black hole. Perhaps surprisingly, it is an infinitely repeating pattern, both to the past and to the future, as shown in Figure 56, where the conformal factor has been chosen so the singularity appears as a vertical line.

6.2.4 Cauchy Horizons: Strong Cosmic Censorship

The Penrose diagram reveals the meaning of the inner horizon $r = r_-$. Consider some initial data specified on a spatial surface Σ , like that shown in Figure 57. Such a surface is referred to as a *Cauchy surface*. We then evolve this initial data forward using the equations of motion.

Sadly, once we encounter a timelike singularity, such evolution is no longer possible, because we need information about what the fields are doing at the singularity. We see that the data on Σ can only be evolved as far as the inner horizon $r = r_-$. The null surface $r = r_-$ is called a *Cauchy horizon*.

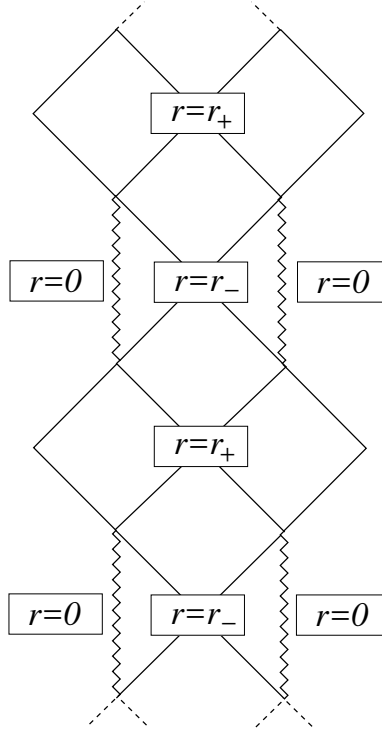


Figure 56: The Penrose diagram for the Reissner-Nordström black hole.

The Cauchy horizon is believed to be unstable. To get some intuition for this, consider the two observers shown in Figure 57. Observer A stays sensibly away from the black hole, sending signals with some constant frequency – say, 1 second – into the black hole for all eternity. Meanwhile, adventurous but foolish observer B ventures into the black hole where he receives the signals. But the signals get closer and closer together as he approaches $r = r_-$, an eternities worth of signals arriving in a finite amount of time, like emails on the first day back after vacation. These signals are therefore infinitely blue shifted, meaning that a small perturbation in the asymptotic region results in a divergent perturbation on the Cauchy horizon.

This instability means that much of the Penrose diagram of the Reissner-Nordström black hole, including the timelike singularity, is unphysical. It is unclear what the end point of the perturbation will be. But, whatever the outcome, you should probably take the Penrose diagram inside the horizon with something of a pinch of salt: if you make it into a black hole interior, your very presence means that it's very unlikely to look like that depicted in this simple idealised case. One possibility is that the Cauchy horizon $r = r_-$ becomes a singularity.

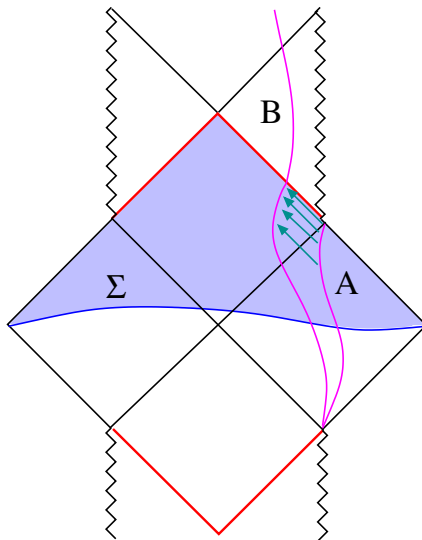


Figure 57: Initial data is specified on Σ , a spatial hypersurface. But this can't be evolved past the *Cauchy horizon*, $r = r_-$, shown as the red line in the figure. The extended geometry for the Reissner-Nordström black hole includes both a future Cauchy horizon, and a past Cauchy horizon.

The instability of the Cauchy horizon is a consequence of a second cosmic censorship conjecture:

The Strong Cosmic Censorship Conjecture: For matter obeying a suitable energy condition, generic initial conditions do not result in a Cauchy horizon. Relatedly, timelike singularities do not form.

Strong cosmic censorship is the statement that general relativity is, generically, a deterministic theory. It is neither stronger nor weaker than weak cosmic censorship and the two, while clearly related, are logically independent. (There is a tradition in general relativity of naming two things “weak” and “strong” even though strong is not stronger than weak.)

6.2.5 Extremal Black Holes

It remains to describe the extremal Reissner-Nordström black hole, with

$$|e| = GM$$

In this case, the inner and outer horizon coalesce and the metric takes the form

$$ds^2 = - \left(1 - \frac{GM}{r}\right)^2 dt^2 + \left(1 - \frac{GM}{r}\right)^{-2} dr^2 + r^2 d\Omega_2^2 \quad (6.25)$$

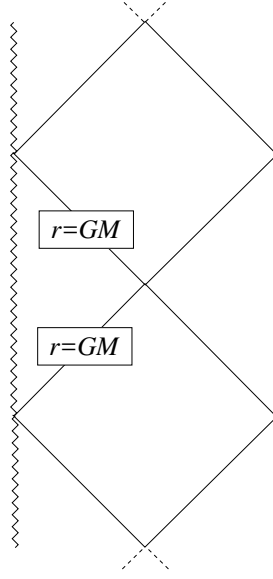


Figure 58: The Penrose diagram for the extremal Reissner-Nordström black hole.

There is just a single coordinate singularity at $r = GM$, but it is now a double pole.

As before, one can use Eddington-Finkelstein coordinates to show that the spacetime can be extended to all $r > 0$, and Kruskal-like coordinates to construct the global causal structure. The resulting penrose diagram is shown in Figure 58.

The extremal black hole has a number of curious features. First, we can look at the spatial distance from a point $r = R$ to the horizon. For a sub-extremal black hole, with an inner and outer horizon, this is given by

$$s = \int_{r_+}^R \frac{dr}{\sqrt{(1 - r_+/r)(1 - r_-/r)}} < \infty$$

However, for the extremal black hole, with $r_+ = r_- = GM$, this becomes

$$s = \int_{GM}^R dr \left(1 - \frac{GM}{r}\right)^{-1} = \infty$$

So the horizon of an extremal black hole lies at infinite spatial distance. In contrast, timelike and null geodesics have no difficulty in reaching the horizon in finite affine parameter.

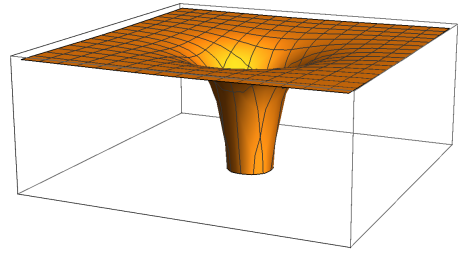


Figure 59:

We should think of the horizon of the black hole as developing an infinite throat as shown in figure; this is what becomes of the Einstein-Rosen bridge, now restricted to just one side.

To understand what the extremal geometry looks like deep within the throat, we can take the near horizon limit. We write

$$r = r_+ + \eta$$

For $\eta \ll GM$, the metric (6.25) takes the form

$$ds^2 = -\frac{\eta^2}{r_+^2} dt^2 + r_+^2 \frac{d\eta^2}{\eta^2} + r_+^2 d\Omega_2^2$$

The first two terms are the metric for the Poincaré patch of two-dimensional anti-de Sitter spacetime (4.28). The final term is just a two-sphere of constant radius. In this way, we see that the near horizon limit of the extremal Reissner-Nordström black hole is $\text{AdS}_2 \times \mathbf{S}^2$; this is sometimes called the *Robinson-Bertotti metric*. Similar calculations to this play an important role in motivating the AdS/CFT correspondence from the dynamics of branes in string theory.

Multi-Black Hole Solutions

If we take, for example, electrically charged black holes, the extremality condition $|e| = GM$ means that $Q_e^2/4\pi = GM^2$. Viewed from a somewhat 17th century perspective, this says that the repulsive Coulomb force between two black holes exactly cancels the attractive Newtonian gravitational force. We may then wonder if it's possible to construct two or more black holes sitting in equilibrium.

The considerations above by no means guarantee the existence of such solutions. It should be clear by now that there's much more to general relativity than a simple $1/r^2$ Newtonian force law, and we still have the seemingly formidable task of solving the non-linear Einstein equations without the crutch of spherical symmetry. Nonetheless, it's at least possible that there exist time independent solutions. This is in contrast to Schwarzschild or sub-extremal Reissner-Nordström black holes, where the attractive force means that two black holes must be orbiting each other, emitting gravitational waves in the process.

Given the complexity of the Einstein equations, it is perhaps surprising that there is not only a time-independent multi-black hole solution, but one that is remarkably simple. To motivate this, we first introduce a new radial coordinate

$$\rho = r - GM$$

Clearly the singularity sits at $\rho = 0$. In this coordinate, the extremal Reissner-Nordström metric (6.25) takes the form

$$ds^2 = -H(\rho)^{-2}dt^2 + H(\rho)^2 (d\rho^2 + \rho^2 d\Omega_2^2) \quad \text{with} \quad H(\rho) = 1 + \frac{GM}{\rho}$$

This form now admits a simple generalisation to

$$ds^2 = -H(\mathbf{x})^{-2}dt^2 + H(\mathbf{x})^2 d\mathbf{x} \cdot d\mathbf{x}$$

where \mathbf{x} is the usual Cartesian coordinate on \mathbf{R}^3 . We further make the ansatz for the gauge field $A = H^{-1}dt$, corresponding to electrically charged black holes. (There is a simple generalisation to black holes carrying both electric and magnetic charge.) Then the non-linear Einstein-Maxwell equations reduce to a very simple linear condition on $H(\mathbf{x})$,

$$\nabla^2 H = 0$$

where ∇^2 is the Laplacian on flat \mathbf{R}^3 . Subject to certain asymptotic boundary conditions this is solved by

$$H(\mathbf{x}) = 1 + \sum_{i=1}^N \frac{1}{|\mathbf{x} - \mathbf{x}_i|}$$

This is the *Majumdar-Papapetrou solution*, discovered in 1947. It describes N black holes sitting at arbitrary positions \mathbf{x}_i .

6.3 Rotating Black Holes

In this section, we turn to rotating black holes. These are the appropriate solutions to describe all black holes observed in the universe.

6.3.1 The Kerr Solution

Rotating objects have an axis of rotation, and this necessarily breaks the rotational symmetry. This makes the solution for rotating black holes considerably more complicated than the spherically symmetric solutions that we have discussed so far.

The solution is written in so-called *Boyer-Lindquist* coordinates (t, r, θ, ϕ) . It takes the form

$$ds^2 = -\frac{\Delta}{\rho^2} (dt - a \sin^2 \theta d\phi)^2 + \frac{\sin^2 \theta}{\rho^2} [(r^2 + a^2)d\phi - a dt]^2 + \frac{\rho^2}{\Delta} dr^2 + \rho^2 d\theta^2 \quad (6.26)$$

where $\Delta(r)$ and $\rho^2(r, \theta)$ are the following functions

$$\Delta = r^2 - 2GMr + a^2 \quad \text{and} \quad \rho^2 = r^2 + a^2 \cos^2 \theta$$

This is the *Kerr solution*, written down in 1963. It's also useful to have an expression for the metric from which we can immediately read off the g_{tt} , $g_{t\phi}$ and $g_{\phi\phi}$ metric components,

$$ds^2 = - \left(1 - \frac{2GMr}{\rho^2} \right) dt^2 - \frac{4GMa r \sin^2 \theta}{\rho^2} dt d\phi + \frac{\rho^2}{\Delta} dr^2 + \frac{\sin^2 \theta}{\rho^2} [(r^2 + a^2)^2 - \Delta a^2 \sin^2 \theta] d\phi^2 + \rho^2 d\theta^2 \quad (6.27)$$

After ploughing through some algebra, you can convince yourself that the Kerr solution has the rather non-obvious property

$$g_{t\phi}^2 - g_{tt}g_{\phi\phi} = \Delta \sin^2 \theta \quad (6.28)$$

We'll make use of this below.

The Kerr solution depends on two parameters: M and a . A quick inspection of the metric shows that a has dimension of length. When $a = 0$, the Kerr solution reduces to the Schwarzschild solution.

Far from the black hole, $r \gg GM, a$, the metric reduces to flat Minkowski spacetime, with (t, r, θ, ϕ) the usual coordinates, with $\theta \in [0, \pi]$ and $\phi \in [0, 2\pi)$.

There are two continuous isometries of the Kerr metric. These are

$$K = \frac{\partial}{\partial t} \quad \text{and} \quad L = \frac{\partial}{\partial \phi}$$

We can compute Komar integrals for each of these, giving the mass and angular momentum of the black hole respectively. Unsurprisingly, it turns out that the mass is M . The Komar integral of the rotational Killing vector L gives the angular momentum

$$J = aM$$

Flipping the sign of a changes the direction of the spin. In what follows, we take $a > 0$ without loss of generality.

The Schwarzschild solution was also invariant under the discrete symmetries $t \rightarrow -t$ and $\phi \rightarrow -\phi$. The Kerr solution is invariant only under the combination $(t, \phi) \rightarrow (-t, -\phi)$, as appropriate for a spinning object.

Black Hole Uniqueness

There are a bunch of theorems, each with slightly different assumptions, that collectively can be summarised as: any time-independent, asymptotically flat black hole solution, lies within the Kerr family. In other words, black holes are characterised by only two numbers: mass M and angular momentum J . (If we are in Einstein-Maxwell theory, these theorems are extended to allow for electric and magnetic charges as well; we'll briefly discuss this in Section 6.3.4.)

These theorems are not as strong as Birkhoff's theorem. There we needed only to assume spherical symmetry to land on the Schwarzschild solution. This ensured that the Schwarzschild metric describes the spacetime outside a star, even one that is undergoing spherical collapse.

In contrast, the wider set of theorems make explicit use of the event horizon. This means that the Kerr solution does not necessarily describe the spacetime outside a rotating star, although it seems plausible that it is a good approximation far from the surface of the star.

Nonetheless, these theorems tell us that the end point of gravitational collapse is generically the Kerr black hole. This is rather surprising. General relativity is a classical theory that can be derived from an action principle. In fact, it turns out that it is a Hamiltonian theory. Basic properties of Hamiltonian systems — like Liouville's theorem — say that the end point of generic evolution can't be a single point in phase space. Instead, that kind of behaviour is what we expect from a non-Hamiltonian systems with friction. In many ways, black holes act like systems with friction. These kinds of issues become even sharper when we bring quantum mechanics into the mix, where they reappear as the *information paradox*.

6.3.2 The Global Structure

When $\Delta = 0$, the g_{rr} component of the metric diverges. Our previous experience with the Schwarzschild and Reissner-Nordström black holes suggests that these are coordinate singularities, and this turns out to be correct. We write the roots of Δ as

$$\Delta = (r - r_+)(r - r_-)$$

with

$$r_{\pm} = GM \pm \sqrt{G^2M^2 - a^2}$$

This has the same structure as the Reissner-Nordström black hole, and we can immediately import some lessons from there. In particular, if the black hole spins too fast,

so $a > GM$, then the Kerr solution exhibits a naked singularity and is disallowed. The fastest spinning black hole has $a = GM$ and, correspondingly, $J = (GM)^2$. This is the extremal Kerr black hole. More generally, the allowed values of spin are $a/GM \leq 1$.

To show that $r = r_{\pm}$ are coordinate singularities, we can do something akin to the Eddington-Finkelstein trick. This time things are a little trickier. We introduce the *Kerr coordinates* (v, r, θ, χ) where $v = t + r_{\star}$ and r_{\star} and χ defined by

$$dr_{\star} = \frac{r^2 + a^2}{\Delta} dr \quad \text{and} \quad d\chi = d\phi + \frac{a}{\Delta} dr \quad (6.29)$$

The idea, once again, is that these coordinates are adapted to null, in-falling geodesics. However, now there are no radial geodesics: instead they get twisted round by the rotation of the black hole. These geodesics don't, therefore, sit at constant ϕ but instead sit at constant χ . To see this, we exchange t and ϕ in favour of v and χ in (6.26) to find

$$ds^2 = -\frac{\Delta}{\rho^2} [dv - a \sin^2 \theta d\chi]^2 + \frac{\sin^2 \theta}{\rho^2} [a dv - (r^2 + a^2)d\chi]^2 + (dv - a \sin^2 \theta d\chi)dr + \rho^2 d\theta^2$$

First, note that null geodesics follow $dv = d\chi = d\theta = 0$ as promised (since this ensures that $ds^2 = 0$.) Second, as with Eddington-Finkelstein coordinates, there is no longer a factor of Δ in the denominator. This ensures that we can now extend the r coordinate down to $r > 0$ without hitting any singularity. We learn that $r = r_{\pm}$ in the original Kerr metric (6.26) were indeed coordinate singularities as advertised.

To build up the full causal structure, we need Kruskal-like coordinates, analogous to the U_{\pm} and V_{\pm} coordinates (6.23) that we introduced for the Reissner-Nordström black hole. The procedure is now the same. The U_+ and V_+ coordinates allow us to extend the spacetime past the outer horizon at r_+ , down to the inner horizon at r_- . We then need to switch to the U_- and V_- coordinates to get down to the singularity. This then repeats itself. The resulting Penrose diagram again repeats ad infinitum, as shown in Figure 60.

The Singularity

There are a number of ways in which the global structure of the Kerr solution differs from Reissner-Nordström. One is the singularity. The g_{tt} component of the Kerr metric diverges when

$$\rho^2 = 0 \quad \Rightarrow \quad r = 0 \quad \text{and} \quad \theta = \frac{\pi}{2}$$

From our experience with the Schwarzschild and Reissner-Nordström black holes, we might expect that this is a true curvature singularity. This is confirmed by an analysis of the Kretschmann scalar.

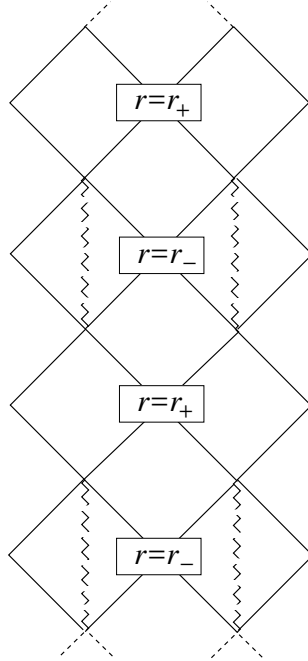


Figure 60: The Penrose diagram for the Kerr black hole.

However, in the previous cases the singularity arose at $r = 0$. There was no need to also specify the angular coordinates on the \mathbf{S}^2 because the \mathbf{S}^2 degenerated at $r = 0$, just like at the origin of flat space. In contrast, the singularity in Kerr occurs only when $\theta = \pi/2$. To better understand this, we can look at the Kerr metric (6.26) at $r = 0$, with constant t : it is

$$ds^2 = a^2 \sin^2 \theta d\phi^2 + a^2 \cos^2 \theta d\theta^2$$

We see that the \mathbf{S}^2 has not degenerated at this point, but nor does it have the round metric. This is to be expected, since the Kerr solution did not have rotational symmetry. The restriction to $\theta = \pi/2$ puts us on the “equator”: this is a ring of radius a , parameterised by $\phi \in [0, 2\pi)$. Thus we learn that the singularity of the Kerr black hole has a ring structure! The singularity is again timelike, as shown in the Penrose diagram.

Strictly speaking, Penrose diagrams can only be drawn for rotationally invariant spacetimes, since we suppress the \mathbf{S}^2 . For Kerr, we compromise and draw the singularity as the jagged, broken line in Figure 60, reflecting the fact that the singularity only occur when $\theta = \pi/2$ and not for other angles on the \mathbf{S}^2 .

Closed Timelike Curves

In the Reissner-Nordström black hole, the spacetime ended at the timelike singularity. But because the \mathbf{S}^2 doesn't degenerate for Kerr, spacetime continues past the singularity (i.e. to the right and left of the timelike singularities shown in Figure 60).

This region can be accessed by observers following a timelike geodesic that passes through $r = 0$ at $\theta \neq \pi/2$. This corresponds to $r < 0$ in the original coordinates of (6.26).

This new region has a weird property: it acts as a time machine! To see this, consider a curve which sits at constant t and r and $\theta = \pi/2$. In other words, the curve is parameterised by ϕ . From (6.26), the metric for this curve is

$$ds^2 = \left(-\frac{a^2\Delta}{r^2} + \frac{(r^2 + a^2)^2}{r^2} \right) d\phi^2 = \left(r^2 + a^2 + \frac{2GMa^2}{r} \right) d\phi^2$$

For $r < 0$ and suitably small, this term in brackets is negative. This means that ϕ is a timelike direction close to the singularity. But ϕ is a periodic coordinate, with ϕ and $\phi + 2\pi$ identified. This means that if you move along this curve, you get back to the same point in time that you started from. This is a *closed timelike curve*.

Having a time machine tucked away inside a black hole is not going to allow you to play Johnny B. Goode at the Enchantment Under the Sea dance. Nonetheless, the idea that time machines arise in the laws of physics is a tantalising one. Sadly, the time machine inside the Kerr black hole is most likely unphysical: it is hidden behind a Cauchy horizon and, as we discussed previously such horizons are unstable to generic perturbations.

Closed timelike curves are not uncommon, and arise in several other solutions to the Einstein equations. Nonetheless, like naked singularities, there is a general belief that they should not form from any sensible initial conditions, a fact referred to the *chronology protection conjecture*.

6.3.3 The Ergoregion

There is also something special about the Kerr black hole outside the horizon. To see this, consider the Killing vector

$$K = \frac{\partial}{\partial t}$$

Far from the black hole, this is a timelike Killing vector. Indeed, asymptotically, at $r \rightarrow \infty$, K generates the geodesics of an observer stationary with respect to the black

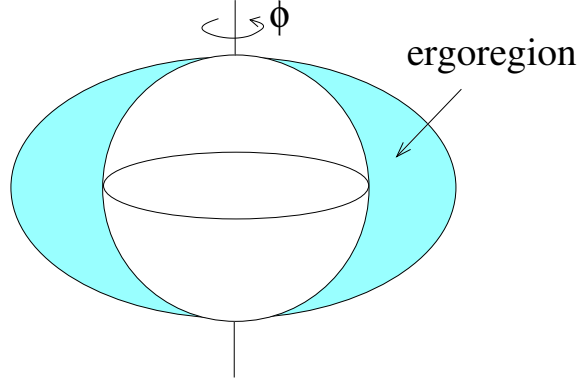


Figure 61: The ergoregion outside the Kerr black hole.

hole. As we move closer to the black hole, with finite r , the integral curves of K are no longer geodesics since they sit at constant r (as well as constant θ and ϕ), but it's always possible to follow these curves by turning on the thrusters on our rocket ship. At some point, however, this ceases to be true.

To see this, we look at the norm of K ,

$$g_{\mu\nu}K^\mu K^\nu = g_{tt} = -\frac{1}{\rho^2} (r^2 - 2GMr + a^2 \cos^2 \theta)$$

This is negative, and hence K is timelike, for large r . However, K becomes null when

$$r^2 - 2GMr - a^2 \cos^2 \theta = 0 \quad \Rightarrow \quad r = GM \pm \sqrt{G^2M^2 - a^2 \cos^2 \theta} \quad (6.30)$$

We should compare this to the horizons, which sit at $r_{\pm} = GM \pm \sqrt{G^2M^2 - a^2}$. The smaller root in (6.30) sits inside the horizon, but the larger root sits outside the horizon, except at the poles $\theta = 0, \pi$ where it touches. We learn that K becomes spacelike in a region outside the horizon,

$$GM + \sqrt{G^2M^2 - a^2} < r < GM + \sqrt{G^2M^2 - a^2 \cos^2 \theta}$$

This is called the *ergoregion*. It is sketched in Figure 61. The outer boundary of the ergoregion is called the *ergosurface*.

Inside the ergoregion, an observer cannot follow integral curves of K because these curves are no longer timelike. This means that, no matter how hard you fire your rocket thrusters, you cannot sit at constant r , θ and ϕ . To see what's happening, let's look again at the Kerr metric

$$ds^2 = -\frac{\Delta}{\rho^2} (dt - a \sin^2 \theta d\phi)^2 + \frac{\sin^2 \theta}{\rho^2} [(r^2 + a^2)d\phi - a dt]^2 + \frac{\rho^2}{\Delta} dr^2 + \rho^2 d\theta^2$$

We want to find a timelike curve, with $ds^2 < 0$. Moving in the r and θ directions do not help, since g_{rr} and $g_{\theta\theta}$ are both positive. In fact, the only negative term comes from $g_{t\phi}$. This means that any timelike trajectory in the ergoregion necessarily requires movement in ϕ .

This is an example of *frame dragging*, albeit an extreme one. In the ergoregion, observers are necessarily swept around by the rotation of the black hole. They can still escape the black hole's clutches should they wish, since they have not yet crossed the outer horizon, but as long as they remain in ergoregion they rotate relative to asymptotic observers.

The Penrose Process

A clever idea, due to Penrose, allows us to extract energy from a rotating black hole. To motivate this, consider again the Killing vector $K = \partial_t$. As we explained in Section 4.3.2, we can use K to assign an energy to any observer with 4-momentum P^μ ,

$$E = -K_\mu P^\mu$$

The 4-momentum is necessarily timelike. If K is also timelike, then the negative sign in the definition above ensures that E is positive. This is because the inner product of two timelike vectors is always negative. However, in the ergoregion K is spacelike, so it is possible for the energy to be negative.

Here, then, is the mechanism to extract energy from a black hole. We send in an object along a geodesic, with 4-momentum P^μ . Because it travels along a geodesic, the energy $E = -K \cdot P$ is conserved and so remains positive even when the object enters the ergoregion.

Once in the ergoregion, we arrange for the object to split into two. (In terms of particle physics, you could imagine a particle decaying although it's rather harder to arrange the details of this before hand.) Conservation of energy and momentum require

$$P = P_1 + P_2$$

and, correspondingly,

$$E = E_1 + E_2$$

But inside the ergoregion, it is possible to arrange things so that $E_1 < 0$. Clearly we must then have $E_2 > 0$. Each of these smaller objects then follows their own geodesic. Because $E_1 < 0$ it is not possible for the first particle to escape the ergoregion; typically,

it will instead fall into the black hole. However, there is no such restriction on the second particle with E_2 and it is possible to arrange things so that this escapes the black hole and comes back to the asymptotic region, now with $E_2 > E$. In other words, the object returns with more energy than it started.

Extracting energy from the black hole means that its mass decreases. (This back-reaction is not included in the calculation above which is done in a fixed background.) If you decrease the mass sufficiently, you might wonder if you can violate the extremality bound to get $J > GM^2$, revealing a naked singularity. Fortunately, this can't happen: a decrease of the mass must be accompanied by a corresponding decrease in the angular momentum.

To see this, consider the combination of Killing vectors

$$\xi = K + \Omega L = \frac{\partial}{\partial t} + \Omega \frac{\partial}{\partial \phi} \quad (6.31)$$

This is also a Killing vector for any constant Ω . We know that K is mostly spacelike on the horizon $r = r_+$. (The exception is at $\theta = 0, \pi$ where the horizon intercepts the ergosurface so K is null.) The angular momentum vector L is also spacelike on the horizon. However, there is a special choice of Ω so that ξ becomes null everywhere on the horizon.

To see this, note that the norm of ξ is

$$\xi^2 = g_{tt} + 2\Omega g_{t\phi} + \Omega^2 g_{\phi\phi}$$

We can make $\xi^2 = 0$ at a general r and θ by taking

$$\Omega(r, \theta) = \frac{-g_{t\phi} \pm \sqrt{g_{t\phi}^2 - g_{tt}g_{\phi\phi}}}{g_{\phi\phi}}$$

If we restrict to the horizon, $r = r_+$ then $\Delta = 0$ and the identity (6.28) tells us that $g_{t\phi}^2 = g_{tt}g_{\phi\phi}$, and we get $\Omega = -g_{t\phi}/g_{\phi\phi}$. A quick look at the metric (6.27) then shows us that the θ dependence drops out, leaving us with the constant

$$\Omega = \frac{a}{r_+^2 + a^2}$$

With this choice of Ω , the Killing vector ξ generates null geodesics on the horizon. The frame dragging now means that these geodesics necessarily rotate in the ϕ direction. We interpret Ω as the angular velocity of the black hole.

We can use ξ to place a restriction on the amount of energy that can be extracted by the Penrose process. The Killing vector ξ is future-pointing, which means that, for any 4-momentum P ,

$$\xi_\mu P^\mu \leq 0 \quad \Rightarrow \quad -E + \Omega j \leq 0$$

where $j = L_\mu P^\mu$ is the angular momentum of the particle. Applying this to the particle with $E_1 < 0$ that falls into the black hole, we have

$$E_1 \geq \Omega j_1 \tag{6.32}$$

In this sense, we necessarily extract more angular momentum than energy from the black hole. To see that this bound does indeed prohibit the formation of super-extremal rotating black holes, consider the following combination

$$A = 8\pi \left[G^2 M^2 + G\sqrt{G^2 M^4 - J^2} \right] = 8\pi GM \left[GM + \sqrt{G^2 M^2 - a^2} \right]$$

If the black hole loses both mass δM and angular momentum δJ , the quantity A changes as

$$\frac{\delta A}{16\pi} = G^2 M \delta M + \frac{G^3 M^3 \delta M - \frac{1}{2} G J \delta J}{\sqrt{G^2 M^4 - J^2}} = \frac{GJ}{2\sqrt{G^2 M^4 - J^2}} \left[\frac{\delta M}{\Omega} - \delta J \right]$$

where, in the second equality, we've used the expression $r_+ = GM + \sqrt{G^2 M^2 - a^2}$, which means that $r_+^2 + a^2 = 2GM(GM + \sqrt{G^2 M^2 - a^2})$. A few lines of algebra then gives the result.

The particle plunging beyond the event horizon results in a reduction of the mass $\delta M = E_1$ of the black hole and a change in the angular momentum $\delta J = j_1$. The inequality (6.32) tells us that $\delta M \geq \Omega \delta J$ and so

$$\delta A \geq 0$$

In other words, A is a quantity which is monotonically increasing in the Penrose process. In particular, this ensures that it's not possible to turn a sub-extremal Kerr black hole into a super-extremal black hole with a naked singularity through the Penrose process.

A Hint of the Area Theorem

The quantity A has a rather special geometric meaning: it is the area of the event horizon of the black hole

$$A = \int_0^\pi d\theta \int_0^{2\pi} d\phi \sqrt{g_{\theta\theta} g_{\phi\phi}} \Big|_{r=r_+} = 4\pi(r_+^2 + a^2) = 8\pi \left[G^2 M^2 + G\sqrt{G^2 M^4 - J^2} \right]$$

where we have evaluated the integral at $r = r_+$, which means that $\Delta = 0$. Our analysis above shows that the area of the black hole always increases.

This is a baby version of a much deeper theorem, proved by Hawking, which says that the area of a black hole increases under all physical processes. Indeed, there is a deep reason behind this: the area of the black hole has the interpretation of entropy, through the famous Bekenstein-Hawking formula

$$S_{BH} = \frac{c^3 A}{4G\hbar}$$

The fact that the area necessarily increases is then part of the generalised second law of thermodynamics.

Superradiance

There is a grown-up version of the Penrose process in which fields scatter off a Kerr black hole, and return amplified. This effect is known as *superradiance*.

Here we sketch this phenomenon for a massless scalar field Φ . The energy-momentum tensor is (4.51)

$$T_{\mu\nu} = \nabla_\mu \Phi \nabla_\nu \Phi - \frac{1}{2} g_{\mu\nu} \nabla^\rho \Phi \nabla_\rho \Phi$$

We know from Section 4.5.5 that we can form a conserved current by contracting $T^{\mu\nu}$ with a suitable Killing vector. In particular, we can measure energy by contracting with $K = \partial_t$ to give the current

$$J^\nu = -K_\mu T^{\mu\nu} = -(K^\mu \nabla_\mu \Phi) \nabla^\nu \Phi + \frac{1}{2} (\nabla^\rho \Phi \nabla_\rho \Phi) K^\nu$$

This obeys $\nabla_\mu J^\mu = 0$.

We now repeat the kind of calculation that we saw in Section 4.5.5. The energy in the field on a spatial hypersurface outside the black hole is

$$E(\Sigma) = \int_\Sigma d^3x \sqrt{\gamma} n_\mu J^\mu$$

with γ_{ij} the pull-back of the metric onto Σ , and n^μ the future-pointing normal. We now integrate $\nabla_\mu J^\mu$ over the shaded region in Figure 62. Assuming that $\nabla\Phi = 0$ at spatial infinity, i^0 , we have

$$0 = \int_V d^4x \sqrt{-g} \nabla_\mu J^\mu = \int_{\Sigma_2} d^3x \sqrt{\gamma_2} n_\mu^2 J^\mu - \int_{\Sigma_1} d^3x \sqrt{\gamma_1} n_\mu^1 J^\mu + \int_{\mathcal{N}} d^3 S_\mu J^\mu$$

with \mathcal{N} the appropriate part of the horizon. Rearranging, we have

$$E(\Sigma_2) - E(\Sigma_1) = - \int d^2A dv \xi_\mu J^\mu$$

where v is the null Kerr coordinate, ξ is the null Killing vector (6.31) along the horizon, and d^2A is the spatial cross-section of the horizon.

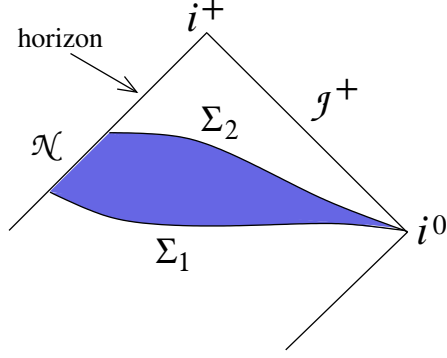


Figure 62: Integrating over a spatial region outside a black hole.

The power absorbed by the black hole per unit null time is then

$$\mathcal{P} = - \int d^2 A \xi_\mu J^\mu$$

with

$$\xi_\mu J^\mu = -(K^\mu \nabla_\mu \Phi)(\xi^\nu \nabla_\nu \Phi) + \frac{1}{2}(\nabla^\rho \Phi \nabla_\rho \Phi)(\xi_\mu K^\mu)$$

The final term vanishes because, when evaluated on the horizon, $\xi \cdot K = 0$. To see this, we evaluate

$$\xi_\mu K^\mu = g_{tt} + \Omega g_{t\phi} \quad \Rightarrow \quad \xi_\mu K^\mu \Big|_{r_+} = \left(g_{tt} - \frac{g_{t\phi}^2}{g_{\phi\phi}} \right)_{r=r_+}$$

But evaluated on the horizon, where $\Delta = 0$, the identity (6.28), tells us that $g_{t\phi}^2 = g_{tt}g_{\phi\phi}$ and so $\xi_\mu K^\mu = 0$. This means that we can write the power as

$$\mathcal{P} = \int d^2 A (K^\mu \nabla_\mu \Phi)(\xi^\nu \nabla_\nu \Phi) = \int d^2 A \frac{\partial \Phi}{\partial v} \left(\frac{\partial \Phi}{\partial v} + \Omega \frac{\partial \Phi}{\partial \chi} \right)$$

We can expand the scalar field in angular momentum modes. In terms of the Kerr coordinates (6.29),

$$\Phi = \Phi_0(r, \theta) \cos(\omega v + \nu \chi)$$

We take the frequency to be positive: $\omega > 0$. Periodicity of χ requires that the angular momentum is quantised, with $\nu \in \mathbf{Z}$. The time averaged power absorbed by the black hole is

$$\bar{\mathcal{P}} = \frac{1}{2} \left[\int d^2 A \Phi_0^2(r_+, \theta) \right] \omega(\omega - \Omega\nu)$$

For high frequency waves, this power is always positive, telling us that the black hole absorbs energy as expected. However, for frequencies small compared to the angular momentum of the ingoing wave,

$$\omega < \Omega\nu$$

the power absorbed is negative. This is the field theoretic version of the Penrose process.

6.3.4 The No Hair Theorem

Uniqueness theorems tell us that the Kerr metric is the most general black hole solution to the vacuum Einstein equations. But what if we add further fields to the action?

We've already seen in Section 6.2 that adding a Maxwell field to the action opens up a new possibility: a black hole solution that carries electric or magnetic charge. There is a generalisation that describes a black hole with both charge and rotation. This amalgam of the Reissner-Nordström and Kerr solutions has metric

$$ds^2 = - \left(1 - \frac{2GMr}{\rho^2} + \frac{e^2}{\rho^2} \right) dt^2 - \frac{2a \sin^2 \theta}{\rho^2} [2GMr - e^2] dt d\phi + \frac{\rho^2}{\Delta} dr^2 \\ + \frac{\sin^2 \theta}{\rho^2} [(r^2 + a^2)^2 - \Delta a^2 \sin^2 \theta] d\phi^2 + \rho^2 d\theta^2$$

where $\Delta(r)$ and $\rho^2(r, \theta)$ now take the form

$$\Delta = r^2 - 2GMr + a^2 + e^2 \\ \rho^2 = r^2 + a^2 \cos^2 \theta \\ e^2 = \frac{G}{4\pi} \sqrt{Q_e^2 + Q_m^2}$$

Meanwhile, the gauge field is given by

$$A = -\frac{Q_e r}{4\pi \rho^2} (dt - a \sin^2 \theta d\phi) - \frac{Q_m \cos \theta}{4\pi \rho^2} (a dt - (r^2 + a^2) d\phi)$$

This is the *Kerr-Newman solution*.

This is the most general black hole solution of the Einstein-Maxwell equations: the black holes are characterised by mass, M , angular momentum J , and electric and magnetic charges Q_e and Q_m . Note that all of these are familiar conserved quantities of classical systems.

What about other fields? It turns out that these cannot take on other time-independent profiles in the presence of a black hole. This is known as the *no hair theorem*. (It is a statement about black holes in asymptotically flat spacetimes; the story is different for black holes in AdS.)

Here we sketch the no hair theorem for a free, massive scalar field Φ . The fact that we're looking for time-independent solutions means that

$$K^\mu \nabla_\mu \Phi = 0 \tag{6.33}$$

where K^μ is a Killing vector that is timelike outside the horizon. (It is $K = \partial_t$ in the usual coordinates.) The action for the scalar field is

$$\begin{aligned} S_{\text{scalar}} &= \int d^4x \sqrt{-g} \frac{1}{2} (-g^{\mu\nu} \nabla_\mu \Phi \nabla_\nu \Phi - m^2 \Phi^2) \\ &= \int d^4x \sqrt{-g} \frac{1}{2} (-g^{tt} \partial_t \Phi \partial_t \Phi - 2g^{ti} \partial_t \Phi \partial_i \Phi - g^{ij} \partial_i \Phi \partial_j \Phi - m^2 \Phi^2) \end{aligned}$$

The fact that we are working in a mixed-signature metric means that the gradient terms come with a mix of signs. However, restricting to time independent configurations (6.33) means that the time derivatives vanish and so $g^{\mu\nu} \nabla_\mu \Phi \nabla_\nu \Phi \geq 0$. In particular, this means that the action is the sum of two terms, each of which is non-positive.

The proof of the no hair theorem in this case proceeds in a similar way to our demonstration of superradiance. We integrate over the spacetime region V outside a black hole, as shown in Figure 62. This region is bounded by two spatial hypersurfaces, Σ_1 and Σ_2 , with normal $n^\mu \sim K^\mu$, the horizon and an asymptotic region. Integrating by parts we have

$$S_{\text{scalar}} = \int_V d^4x \sqrt{-g} \frac{1}{2} \Phi (+g^{\mu\nu} \nabla_\mu \nabla_\nu \Phi - m^2 \Phi) - \int_{\partial V} d^3x \sqrt{-\gamma} n^\mu \Phi \nabla_\mu \Phi$$

The first, bulk, term vanishes for any Φ that solves the equation of motion. That leaves the second, boundary, term. This vanishes on the two spatial hypersurfaces by dint of (6.33). It also vanishes on the horizon for the same reason, since the normal to the horizon is K^μ the timelike Killing vector. That just leaves the asymptotic region. For asymptotically flat spacetimes, it's not too hard to show that $\Phi \sim 1/r$ as $r \rightarrow \infty$, which is fast enough to ensure that there's no contribution from infinity.

The upshot of this argument is that, when evaluated on a time-independent solution to the equation of motion, we have $S_{\text{scalar}} = 0$ when integrated over any region V of a black hole spacetime. Furthermore, S_{scalar} is the sum of two non-positive terms, so each

of these terms must individually vanish. When $m \neq 0$, we have $m^2\Phi^2 = 0$ so the only solution is the trivial one $\Phi = 0$. (When $m^2 = 0$, we have $\partial_i\Phi = 0$, so any $\Phi = \text{constant}$ is allowed.) This is the no hair theorem: the field Φ cannot develop a static profile in the presence of a black hole.